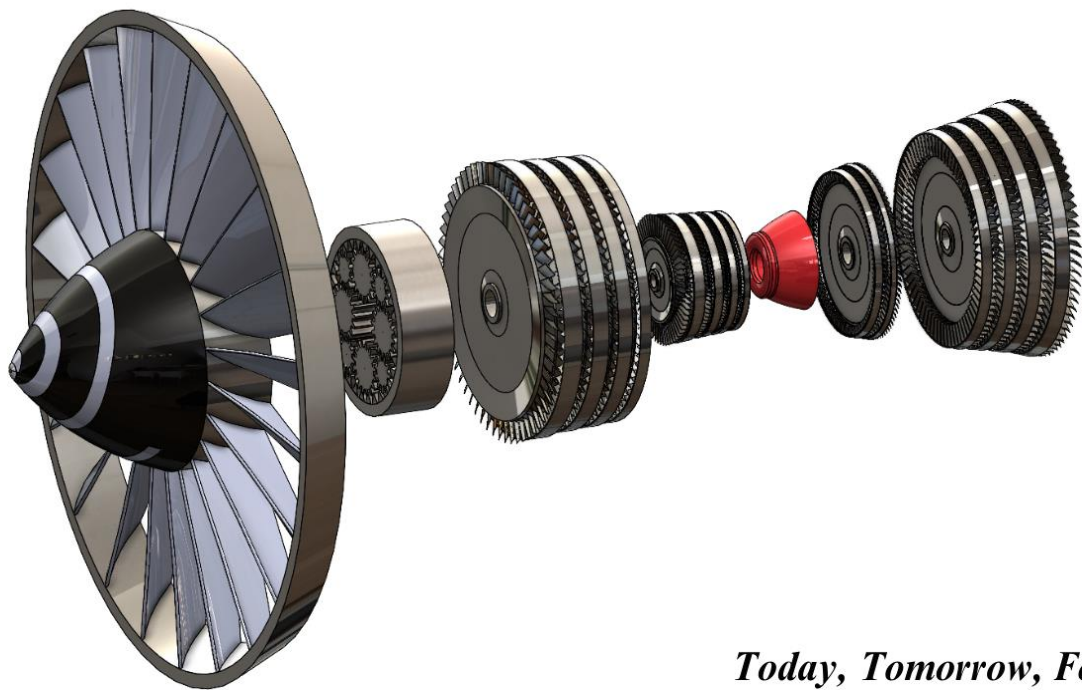




THE CENTURY

A Hybrid-Electric Propulsion System Using Fuselage Boundary Layer Ingestion for a Single Aisle Commercial Aircraft



Today, Tomorrow, Forever...



Signatures



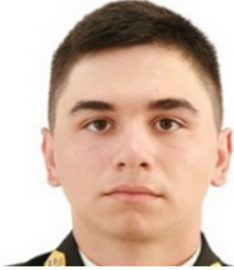
FACULTY ADVISOR

ASST. PROF. DOGUS OZKAN
AIAA MEMBER ID: #1340673
NATIONAL DEFENCE UNIVERSITY TURKISH
NAVAL ACADEMY MECHANICAL ENGINEERING
DEPARTMENT



TEAM LEADER

BURAK UZULMEZ
AIAA MEMBER ID: #1403176
NATIONAL DEFENCE UNIVERSITY TURKISH NAVAL ACADEMY
NAVAL ARCHITECTURE AND MARINE ENGINEERING
DEPARTMENT



TEAM MEMBER

GOKTUG KARACA
AIAA MEMBER ID: #1403589
NATIONAL DEFENCE UNIVERSITY TURKISH NAVAL
ACADEMY MECHANICAL ENGINEERING DEPARTMENT



TEAM MEMBER

MEHMET ADNAN KARAGOZ
AIAA MEMBER ID: #1403277
NATIONAL DEFENCE UNIVERSITY TURKISH NAVAL
ACADEMY MECHANICAL ENGINEERING DEPARTMENT



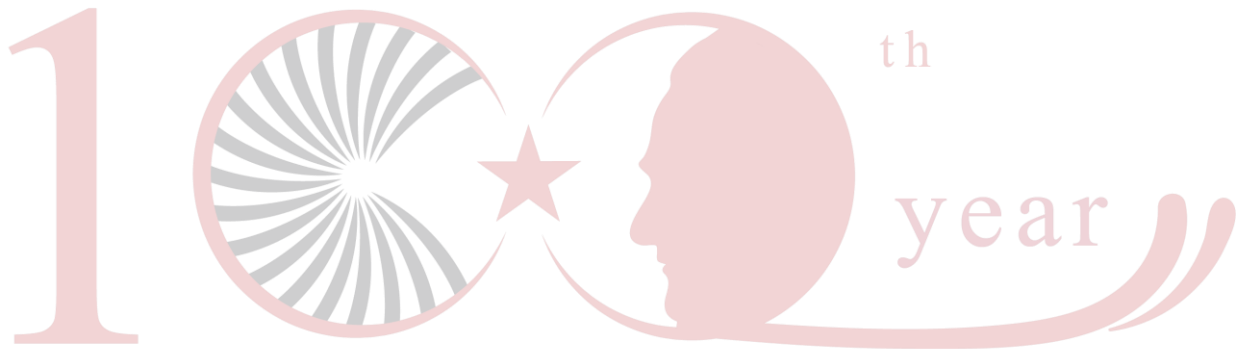
TEAM MEMBER

MEHMET DEMIR
AIAA MEMBER ID: #1403202
NATIONAL DEFENCE UNIVERSITY TURKISH NAVAL
ACADEMY MECHANICAL ENGINEERING DEPARTMENT

TABLE OF CONTENT

NOMENCLATURE AND UNITS	5
ABBREVIATIONS	6
LIST OF FIGURES	7
LIST OF TABLES	8
1 INTRODUCTION	10
2 METHODOLOGY	11
3 DESIGN OF THE CFM-56 BASELINE ENGINE	11
4 ENGINE SELECTION BASED ON PERFORMANCE CYCLE AND MISSION EVALUATION	13
4.1 PERFORMANCE CYCLE EVALUATIONS	13
4.2 Mission Evaluation	15
5 DESIGN OF THE CENTURY-250 ENGINE	17
5.1 PERFORMANCE CYCLE DESIGN AND ANALYSIS	18
6 ENGINE COMPONENT DESIGN	21
6.1 FAN DESIGN	21
6.1.1 OFF-DESIGN ANALYSIS OF FAN	22
6.1.2 FAN BLADE MATERIALS	23
6.2 COMPRESSORS DESIGN	23
6.2.1 LOW PRESSURE COMPRESSOR (LPC) DESIGN	24
6.2.1.1 OFF-DESIGN ANALYSIS OF LPC	25
6.2.1.2 LPC MATERIAL	26
6.2.2 HIGH PRESSURE COMPRESSOR (HPC) DESIGN	26
6.2.2.1 OFF-DESIGN PERFORMANCE OF HPC	28
6.2.2.2 HPC MATERIALS	28
6.3 COMBUSTION CHAMBERS	29
6.3.1 Combustion Chambers Material	29
6.4 TURBINE DESIGNS	29
6.4.1 HIGH PRESSURE TURBINE (HPT) DESIGN	29
6.4.1.1 HPT RESULTS	31
6.4.1.2 OFF-DESIGN PERFORMANCE OF HPT	32

6.4.1.3	HPT MATERIALS	32
6.4.2	LOW PRESSURE TURBINE (LPT) DESIGN.....	33
6.4.2.1	LPT RESULTS	34
6.4.2.2	OFF-DESIGN PERFORMANCE OF LPT.....	35
6.4.2.3	LPT MATERIALS	35
6.5	COLD AND HOT NOZZLE DESIGN	35
6.6	AFT FAN DESIGN.....	36
7	ENGINE WEIGHT AND GEARBOX WEIGHT CALCULATIONS	36
8	HYBRID PROPULSION SYSTEM DESIGN	38
9	MISSION AND PROPULSION COMPARISON.....	40
10	CONCLUSIONS	41
11	REFERENCES	42
12	APPENDIXES	44



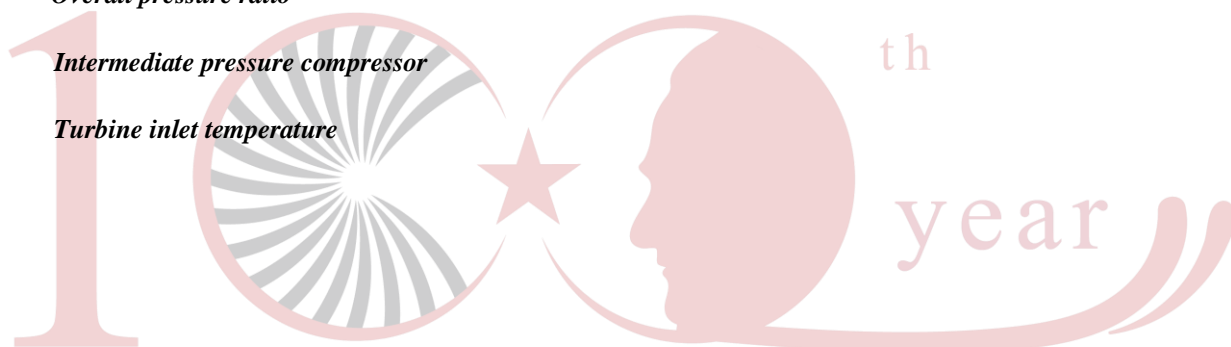
NOMENCLATURE AND UNITS

<i>Description</i>	<i>Unit</i>
\dot{m} <i>Mass flow rate</i>	<i>lb/s</i>
T_a <i>The temperature of the air</i>	<i>R</i>
P_a <i>The pressure of air</i>	<i>psi</i>
$T_{HPT,in}$ <i>High pressure turbine inlet temperature</i>	<i>R</i>
$T_{LPT,in}$ <i>Low pressure turbine inlet temperature</i>	<i>R</i>
$T_{LPT,in}$ <i>Low pressure turbine inlet pressure</i>	<i>psi</i>
<i>TSFC</i> <i>Thrust Specific Fuel Consumption</i>	<i>lb/(lb.h)</i>
ρ <i>Density</i>	<i>lb/in³</i>
U <i>Rotor Speed</i>	<i>ft/s</i>
$r_{hub t}$ <i>Turbine hub radius</i>	<i>in</i>
$r_{hub f}$ <i>Fan hub radius</i>	<i>in</i>
$r_{tip t}$ <i>Turbine tip radius</i>	<i>in</i>
\dot{m}_h <i>Hot mass flow</i>	<i>lb/s</i>
$r_{tip f}$ <i>Fan tip radius</i>	<i>in</i>
ω <i>Angular velocity</i>	<i>ft/s</i>
α_3 <i>Rotor Outlet Angle</i>	<i>°</i>
γ <i>The ratio of the specific heat coefficient</i>	
f <i>Air fuel ratio</i>	
η_c <i>Compressor Efficiency</i>	
ϕ <i>Flow Coefficient</i>	
λ_n <i>Stator loss coefficient</i>	
Ψ <i>Work Coefficient</i>	
A <i>Degree of reaction</i>	
η_t <i>Turbine efficiency</i>	

η_f	<i>Fan efficiency</i>
η_m	<i>Mechanical efficiency</i>
η_j	<i>Hot and cold nozzle efficiency</i>

ABBREVIATIONS

BPR	<i>By-Pass Ratio</i>
FPR	<i>Fan pressure ratio</i>
LPT	<i>Low Pressure Turbine</i>
HPT	<i>High Pressure Turbine</i>
LPC	<i>Low Pressure Compressor</i>
HPC	<i>High Pressure Compressor</i>
OPR	<i>Overall pressure ratio</i>
IPC	<i>Intermediate pressure compressor</i>
TIT	<i>Turbine inlet temperature</i>



LIST OF FIGURES

Figure 1 Cycle calculation results of the CFM56-7B24 engine (a) takeoff condition (on design), (b) cruise condition (off design).....12

Figure 2 Thermodynamic, kinetic, and geometric results of the stations at takeoff condition12

Figure 3 Thermodynamic, kinetic, and geometric results of the stations at cruise condition.....12

Figure 4 CFM56-7B24 Geometry13

Figure 5 Turbofan engine station numbering and engine configuration15

Figure 6 (a) Mission profile, (b) Fuel consumption of selected engine for mission profile.....15

Figure 7 The Century-250 turbofan engine.....18

Figure 8 Parametric study results (a) BPR, TIT (T4) vs SFC, Thrust, (b) OPR vs SFC FPR, BPR (c) MFR vs SFC, BPR, OPR, Thrust19

Figure 9 Cycle results of the Century-250 (a) Take off condition, (b) Cruise condition20

Figure 10 Thermodynamic, kinetic, and geometric results of the stations (a) takeoff condition (b) cruise condition21

Figure 11 Axial fan 2D streamline calculation result (a) relative Mach number, (b) Total temperature, (c) Total pressure22

Figure 12 On and off design performance of the fan.....23

Figure 13 3-D CAD drawing of the fan.....23

Figure 14 2D Streamline calculation results of the LPC, (a) Relative Mach number, (b) Total temperature, (c) Total pressure25

Figure 15 Performance map of the LPC at the cruise and take off conditions26

Figure 16 3-D CAD drawing of the LPC.....26

Figure 17 2D Streamline calculation results of the HPC (a) Relative Mach, (b)Total Temperature and (c)Total Pressure27

Figure 18 Performance map of HPC at cruise and take off conditions28

Figure 19 3-D CAD drawing of the HPC.....29

Figure 20 HPT 2D Flow path calculation result (a) Mach number, (b) Total temperature, (c) Total pressure.....30

Figure 21 Hub section HPT velocity triangles from AxStream31

Figure 22 3-D CAD drawing of the HPT32

Figure 23 HPT off design performance map32

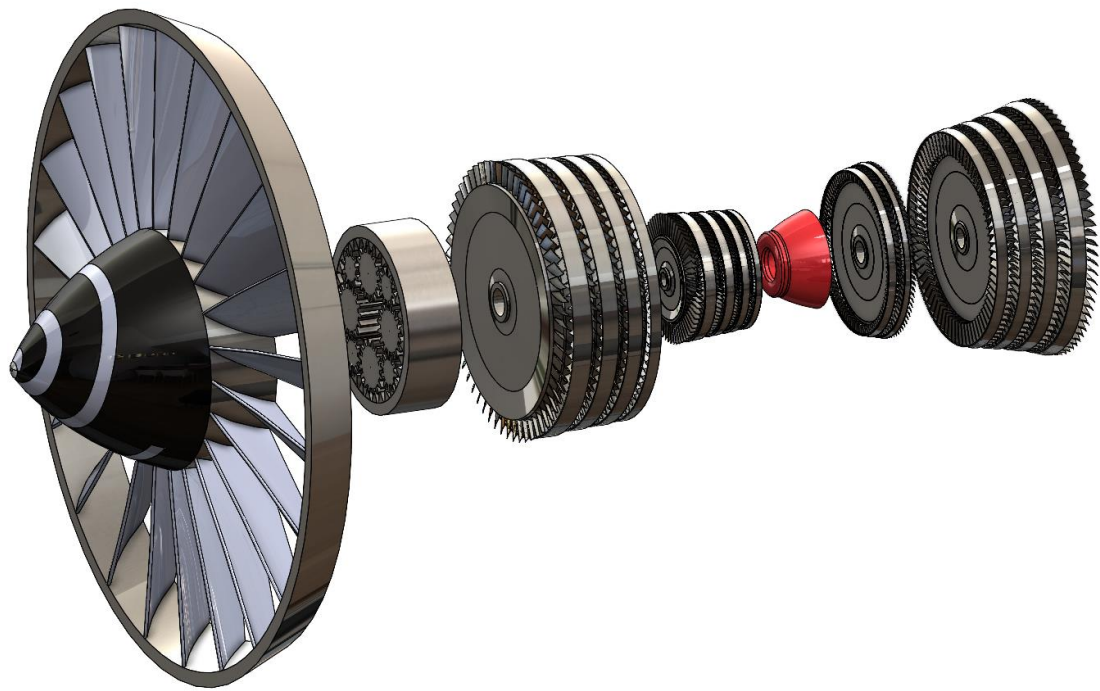
Figure 24 HPT blade material and coatings32

Figure 25 LPT 2D streamline calculation result (a) Relative mach, (b) Total temperature, (c) Total pressure.....33

<i>Figure 26 LPT velocity triangles from AxStream.....</i>	<i>34</i>
<i>Figure 27 3-D CAD drawing of the LPT.....</i>	<i>34</i>
<i>Figure 28 LPT off design performance map.....</i>	<i>35</i>
<i>Figure 29 HPT and LPT smith charts.....</i>	<i>35</i>
<i>Figure 30 AFT fan 2D streamline calculation result (a) Relative mach, (b) Total temperature, (c) Total pressure.....</i>	<i>36</i>
<i>Figure 31 AFT Fan geometry and dimensions from AxStream.....</i>	<i>36</i>
<i>Figure 32 Engine weight and dimensions.....</i>	<i>37</i>
<i>Figure 33 Engine cross section with CFM56-7B24.....</i>	<i>38</i>
<i>Figure 34 Operation of the hybrid-electric propulsive system.....</i>	<i>38</i>
<i>Figure 35 Specifications of the hybrid-electric propulsion system.....</i>	<i>39</i>

LIST OF TABLES

<i>Table 1 CFM56-7B24 engine specifications.....</i>	<i>11</i>
<i>Table 2 Turbofan engine BPR ranges.....</i>	<i>13</i>
<i>Table 3 The engine design parameters for the base and the new engines.....</i>	<i>14</i>
<i>Table 4 Flight mission for CFM56-7B24.....</i>	<i>16</i>
<i>Table 5 Fan design results.....</i>	<i>22</i>
<i>Table 6 Typical axial compressor design parameters used in the literature.....</i>	<i>24</i>
<i>Table 7 Geometric and boundary layer parameters of the LPC.....</i>	<i>24</i>
<i>Table 8 AxStream design results of the LPC.....</i>	<i>25</i>
<i>Table 9 Boundary condition and geometric data used in HPC design.....</i>	<i>26</i>
<i>Table 10 Design results of the HPC.....</i>	<i>28</i>
<i>Table 11 Thermodynamic and geometrical design parameters of the LPT.....</i>	<i>33</i>
<i>Table 12 LPT design results.....</i>	<i>34</i>
<i>Table 13 Net thrust comparison of the baseline and hybrid electric propulsion.....</i>	<i>39</i>
<i>Table 14 Flight mission for designed Century-250 with hybrid electric propulsion system.....</i>	<i>40</i>



1 INTRODUCTION

In recent years, the depletion of fossil fuels and the search for alternative fuel systems has become one of the most important research and innovation topics [1]. Therefore, reducing fuel consumption in internal combustion engines is a crucial factor in achieving energy-efficient power systems and lowering carbon footprints [2]. Hybrid power systems, which combine an internal combustion engine and an electric motor, provide an excellent solution for reducing fuel consumption and emissions from fossil fuels [3]. Therefore, the conversion of internal combustion engines to hybrid systems has increased significantly in the automotive industry in the last decade. Furthermore, the marine industry has been on the way to hybrid propulsion transformation in ships to reduce emissions originating from fossil fuels [4]. Following this, the aviation industry has been working on hybrid-propelled planes to reduce emissions from gas turbines. STARC-ABL is the first passenger plane that has been worked on to be the first hybrid-propelled plane. The propulsion system of the STARC-ABL aircraft is based on a turbo-electric system, which uses electric motors powered by gas turbines mounted under the wings to generate thrust. The basic operating principle of the STARC-ABL aircraft is to reduce drag and take advantage of the slow airflow near the body of the aircraft. This slow airflow is sucked through an aft electric fan mounted on the tail, providing additional thrust, which means more thrust with less fuel consumption. However, the overall SFC decrease is very scant in this configuration. On the other hand, the boundary layer around the aircraft body is ingested by the electrically driven aft fan which hinders a lower level of drag exertion on the body. Thus, a more environment-friendly propulsion system will be achieved with a hybrid propulsion system. In this project, as we are The Century team, we redesigned and made a hybrid propulsion configuration for the STARC-ABL aircraft. CFM56-7B24 engine was used as a baseline engine whose bypass ratio (BPR), turbine inlet temperature (TIT), overall pressure ratio (OPR), and fan pressure ratio (FPR) were revised and optimized via parametric studies. All the designs of the hybrid engine propulsion system were performed through the GasTurb14 software. AxStream was used to design engine components and the aft fan with 1D and 2D thermodynamic/kinetic calculations. With this project, the baseline engine upgraded to new BPR, TIT, FPR, and OPR ratios, and engine TSFC decreased by 7.4% with a 11% thrust increase at the end of the base engine redesign. Hybrid electric propulsion increased the total thrust of the plane by 10% decreased the fuel consumption 20% with degree of hybridization (DOH) of 0.28 with almost similar propulsion system weight when compared to CFM56-7B24 engine.

2 METHODOLOGY

CFM56-7B24 turbofan engine was selected as a baseline engine to redesign and optimization. The engine specifications are given in Table 1[16].

Table 1 CFM56-7B24 engine specifications

PARAMETER	VALUE
Engine Type	Turbofan
Number of Compressor Stages (Fan, LP, HP)	1,3,9
Number of HP/LP Turbine stages	1,4
Combustor Type	Axial annular
Maximum Net Thrust at Sea Level (lbf)	24000lbf
Specific Fuel Consumption at Max. Power (lbm/hr/lbf)	0.37 lbm/hr/lbf
Overall Pressure Ratio at Max. Power	26
Bypass Ratio at Max. Power	5.3
Max. Envelope Diameter (in)	65 in
Max. Envelope Length (in)	98 in
Dry Weight Less Tailpipe (lbm)	5.234 lbm

According to the requested proposal high-pressure compressor (HPC) exit temperature (T_3) and TIT (T_4) was limited to 1620 R and 3150 R, respectively. Here, we designed four different engines by parametric studies based on different optimized BPR, OPR, FPR, MFR, and TIT values. During these studies engine dimensions, engine mass, thrust, and specific fuel consumption (SFC) were taken into consideration. We especially tried not to pass 65-inch diameter and 98-inch length in our engine designs. Aft and fore fans were designed as a single stage by using AxStream. 2D flow path designed and optimized via efficiency, power, and mass-flow rate under 500 iterations. Inlet and outlet thermodynamic and kinetic properties were achieved and presented in the result section. Similarly, compressors and turbines were also designed by using AxStream based on the GasTurb14 data. In this project, The Century team presented the optimal turbofan and electrical cycles based on technological advancements up to 2035. Engine designs were carried out to optimize power delivery, specific fuel consumption, and engineering costs.

3 DESIGN OF THE CFM-56 BASELINE ENGINE

In this project, CFM56-7B24 was selected as a base line engine and the new engines designed based on CFM56-7B24 parameters. Before starting a new engine design, we validated on and off designs of the CFM56-7B24 engine in Gasturb14. Fig. 2 shows baseline engine on and off design cycle calculation results. The trust of 24227lb and a TSFC of 0.3637 lb/(lb.h) was found for takeoff condition (see Fig. 1(a)) whereas these values were found to be 5585lb and 0.6864 lb/(lb.h) for cruise condition (see Fig. 1(b)). BPR and OPR 5.3 and 26 for the baseline engine. Similar isentropic efficiencies were taken with proposal request and the efficiencies of the turbines were calculated by Gasturb14. Thermodynamic, kinetic, and geometric results of the stations at takeoff condition were shown in Fig.2. The Mach number was found to be 0.81 at the exit of the hot nozzle and 0.9 for the cold nozzle. The Mach numbers were 1 for both nozzles at the cruise condition (see Fig. 3).

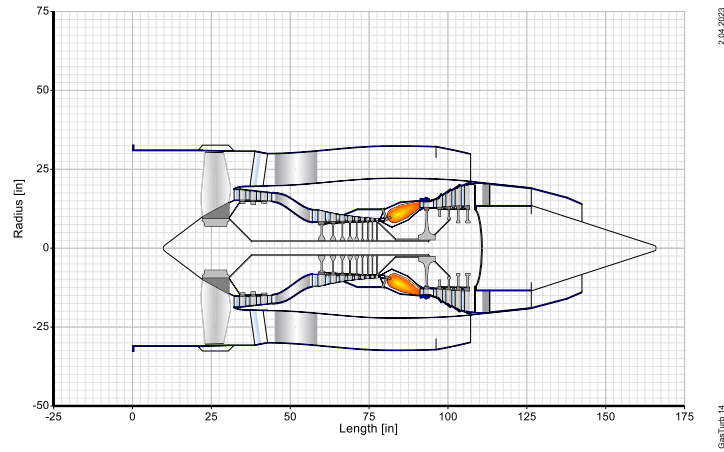


Figure 4 CFM56-7B24 Geometry

4 ENGINE SELECTION BASED ON PERFORMANCE CYCLE AND MISSION EVALUATION

4.1 PERFORMANCE CYCLE EVALUATIONS

An optimal cycle of the new CFM56-7B24 base engine was achieved via more than a million iterations and optimization of TIT, BPR, OPR, and mass flow rate (MFR) in the GasTurb14 software. BPR is one of the important design parameters for turbofan engines that affecting directly cold thrust and SFC. BPRs and their classifications used in turbofan engines were shown in Table 2[24]. The engines were designed on high and ultra-high BPR twin spools without a geared axial fan. The engine consists of a single-stage fan, three gear ratio of gearbox, four stages of low-pressure axial flow compressor, four stages of high-pressure axial flow compressor, a two-stage high-pressure axial turbine, and four stages of low-pressure axial turbine, cold and hot nozzles.

Table 2 Turbofan engine BPR ranges

TYPE OF TURBOFAN ENGINE RANGE OF BPR	
Low-Bypass	$BPR < 2$
Medium-Bypass	$2 \leq BPR \leq 5$
High-Bypass	$5 \leq BPR \leq 9$
Ultra-High-Bypass	$9 \leq BPR$

In this project, four engines were designed with the targets of achieving a minimum thrust of 24,200 lb, a specific fuel consumption (SFC) lower than 0.37 lb/lbf.h at the takeoff condition and 5500lb thrust and a lower SFC than 0.68 lb/lbf.h at the cruise condition for the baseline engine of CFM56-7B24, and a mass lower than 5234 lbm. To achieve these targets, the engines were designed with parametric studies that involved changing and optimizing the OPR, TIT, BPR, HPC exit temperature (T_3), and MFR. During the iterations and optimizations, the maximum compressor exit temperature (T_3) and turbine inlet temperature (T_4) was assumed as 1620R and 3150R, respectively. The design parameters and results of the new engines were shown in Table 3.

Table 3 The engine design parameters for the base and the new engines

Mission	ENGINE 1		ENGINE 2		ENGINE 3		ENGINE 4	
	Take-Off	Cruise	Take-Off	Cruise	Take-Off	Cruise	Take-Off	Cruise
Thrust (lb)	25536	4283	24601	3953	30268	5418	31491	5711
TSFC (lb/(lb*h))	0.21	0.58	0.18	0.59	0.25	0.62	0.23	0.6
Mass Flow (lb/s)	867	341	983	434.4	1338	515	1485	649
T3(R)	1603	1384	1620	1562	1607	1389	1587	1586
T4(R)	3090	3090	2995	3070	3000	3000	3050	3112
V18/V8	0.63	0.41	0.75	0.4	0.43	0.37	0.65	0.37
BPR	11.77	11.77	14.98	15.73	12	12.14	15	16.11
OPR	39.35	39.35	38.4	48.71	39.58	38.9	37.88	46.82
FPR	1.7	1.7	1.26	1.24	1.68	1.66	1.6	1.47
LPC PR	1.58	1.58	1.61	1.91	4.0	3.93	4	5.35
HPC PR	14.88	14.88	19.25	21	6.0	6.15	6.1	6.06
LP Spool Speed	5051	5051	4461	5353	3476	3439	3362	4397
IPC Spool Speed	-	-	-	-	10428	10316	11766	15390
HP Spool Speed	20919	20923	18613	18613	23533	235357	22238	22238
Core Efficiency	0.49	0.57	0.46	0.55	0.49	0.57	0.49	0.57
Prop Efficiency	-	0.79	-	0.84	-	0.82	-	0.85

The main objectives focused on in Engine 1 were to reduce weight and shorten the length of the engine. In line with the objectives, the design process, the bypass ratio (BPR) was kept between 5 and 15 due to its effect on the engine diameter, and a value of 11.77 was deemed appropriate because of optimization studies. At the same time, other objectives were not neglected, and good progress was made in terms of fuel efficiency. In Engine 1, 43% less fuel consumption was achieved at take-off when compared to the baseline engine. The TIT value of 3090R was selected for T4 and 1603R for T3 at on design with 867lb/s mass flow rate. As a result of the optimization studies and iterations, the thrust value was increased by 5.52% to 25536 lb for takeoff. The thrust was increased by %4.35 with 5824lb whereas the decrease in SFC was %23.5 in cruise conditions. Performance cycle results for takeoff and cruise conditions of the Engine 1 were given in appendix 1. Engine 1 was not chosen as a potential candidate for the high-pressure compressor (HPC) with a higher-pressure ratio. This was because the desired pressure ratio of 14.88 for the HPC would require at least 13 stages, and in fact Engine 1's HPC did not have enough stages to achieve this pressure ratio. It is worth noting that in general, one stage of an axial compressor typically has a pressure ratio between 1.2 and 1.4 [24]. Besides, 13 stage of HPC would increase the engine length and weight. Similar to Engine 1 the main goal focused on in the Engine 2 was to maintain the T4 and T3 values at the maximum limits, hence T4 and T3 were found as 2995R and 1620R. The remaining parameters were optimized to provide the necessary thrust at the most optimum values with the least fuel consumption. In line with these goals, the optimum value for the higher BPR values was found to be 14.98 because of less fuel consumption. In addition, an OPR of 38.4 was preferred in engine 2 compared to the baseline engine. As a result of the optimization studies and iterations, the thrust of engine 2 was identical with the baseline engine with 24601 lb, and the fuel consumption has been reduced by 51.3% to 0.18 at the takeoff condition. The performance cycle results for takeoff and cruise conditions of the Engine 2 were shown in appendix 2. However, thrust of engine 2 decreased 16.9% with 4634 lb, whereas TSFC increase was 23.5% at the cruise condition. The engine 1 and 2 were ungeared engines and when we connected the electrical power unit, engines lost too much thrust because of the lower rotational speeds of LP spools. Therefore, we decided to increase rotational speed of the IP spool up to 10000 rpm by using gearbox. For these reasons, engine 3 and 4 were designed with BPRs of 12 and 15 with gear boxes which had a 3:1 and 3.5:1 gear ratio, respectively. Thus, the pressure ratios of LPC and HPC were decreased as well as stage number of the HPC that provide decrement in the engine weight and length. When we increased the intermediate pressure spool rotational speed, we

found that thrust increased to 30268 lb with BPR of 12. Besides TSFC was 0.25 with 32.4% decrement when compared to baseline engine. Furthermore, OPR of the engine was 39.58 which consisted of 1.68 FPR, 4 LPC PR, and 6 HPC PR. On the other hand, cruise thrust increased by 34.7% by using 11377 rpm IP spool rotational speed. However, MFR was increased from 751 lb/s to 1338 lb/s which resulted fan diameter increase. BPR of 15 was chosen for engine 4 with T3 and T4 temperatures of 1587R and 3050R, respectively. The optimum OPR was found to be 37.8 with IP spool rotational speed of 11766 rpm. These parameters provided extraordinary thrusts of 31491lb and 5711lb at the takeoff and cruise conditions. The performance cycle results for takeoff and cruise conditions of the Engine 4 were shown in appendix 3 Results showed that TSFC of engine was similar to engine 3.

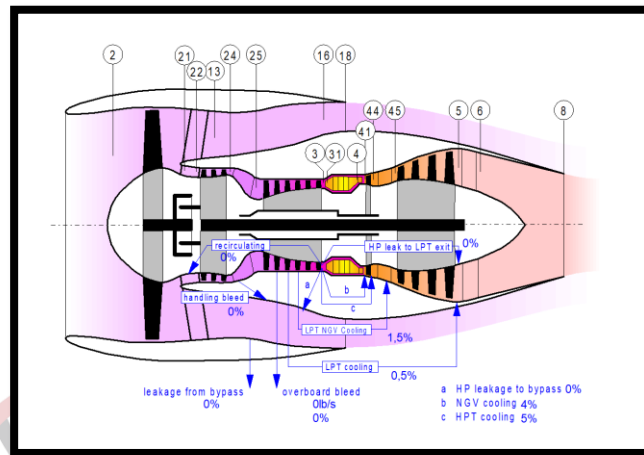


Figure 5 Turbofan engine station numbering and engine configuration

4.2 Mission Evaluation

A mission was planned to test hybrid propulsion system for designed engines in section 3.1. Therefore, a flight from Istanbul airport to San Diego International airport was planned to test the propulsion systems. The graph of the flight mission and fuel consumption were shown in Fig. 5.

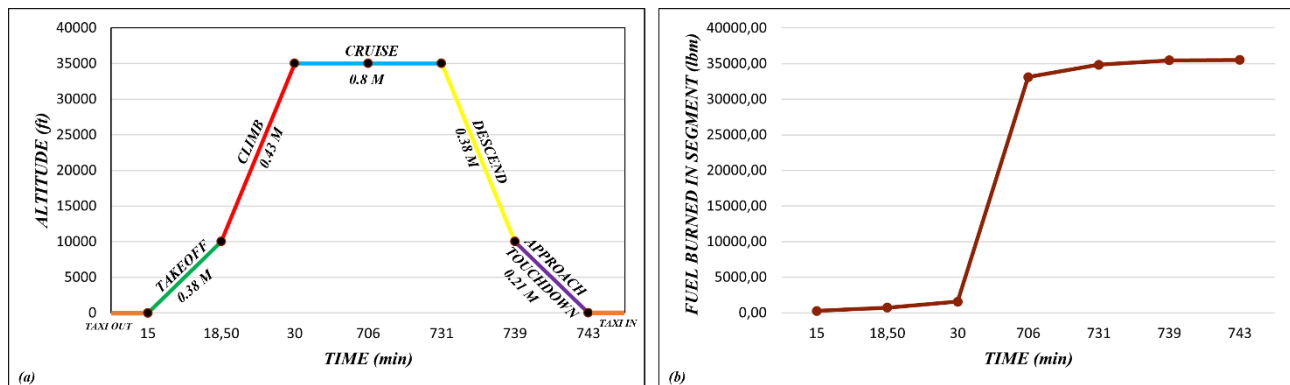


Figure 6 (a) Mission profile, (b) Fuel consumption of selected engine for mission profile

The total flight time 742.7 min including taxi out, takeoff, climb, cruise, descend, approach and taxi in. The mission flight data for baseline engine and four engines were given in Table 4-8. Cruise speed and altitude of the plane were 0.8 Mach and 35000 feet.

Table 4 Flight mission for CFM56-7B24

Segment	Altitude (ft)	Mach Number	Thrust (lbf)	TSFC (lbm/lbf*h)	Fuel Flow (lb/s)	Time(min)	Fuel Burned in Segment (lbm)
Taxi Out	0	0.015	3000	0.42	0.356	15	320.4
Take Off	0-10000	0.38	18000	0.53	2.666	3.5	559.8
Climb	10000-35000	0.43	10000	0.5	1.408	11.5	971.52
Cruise	35000	0.8	5000	0.65	0.910	676.2	36920.52
Descend	35000-10000	0.38	10000	0.48	1.341	24.5	1971.27
Approach & Touchdown	10000-0	0.21	14000	0.44	1.707	8	819.36
Taxi In	0	0.015	3000	0.42	0.356	4	85.44
Total						742.7	41648.31

Table 5 Flight mission for designed engine 1

Segment	Altitude (ft)	Mach Number	Thrust (lbf)	TSFC (lbm/lbf*h)	Fuel Flow (lb/s)	Time(min)	Fuel Burned in Segment (lbm)
Taxi Out	0	0.015	3000	0.29	0.246	15	221.4
Take Off	0-10000	0.38	18000	0.403	2.015	3.5	423.15
Climb	10000-35000	0.43	10000	0.41	1.140	11.5	786.6
Cruise	35000	0.8	5000	0.5	0.707	676.2	28684.4
Descend	35000-10000	0.38	10000	0.38	1.081	24.5	1589.07
Approach & Touchdown	10000-0	0.21	14000	0.32	1.246	8	598.08
Taxi In	0	0.015	3000	0.29	0.246	4	59.04
Total						742.7	32361.74

Table 6 Flight mission for designed engine 2

Segment	Altitude (ft)	Mach Number	Thrust (lbf)	TSFC (lbm/lbf*h)	Fuel Flow (lb/s)	Time(min)	Fuel Burned in Segment (lbm)
Taxi Out	0	0.015	3000	0.308	0.257	15	231.3
Take Off	0-10000	0.38	18000	0.404	2.023	3.5	424.83
Climb	10000-35000	0.43	10000	0.409	1.138	11.5	785.22
Cruise	35000	0.8	5000	0.519	0.721	676.2	29252.41
Descend	35000-10000	0.38	10000	0.386	1.073	24.5	1577.31
Approach & Touchdown	10000-0	0.21	14000	0.314	1.221	8	586.08
Taxi In	0	0.015	3000	0.308	0.257	4	61.68
Total						742.7	32918.83

Table 7 Flight mission for designed engine 3

Segment	Altitude (ft)	Mach Number	Thrust (lbf)	TSFC (lbm/lbf*h)	Fuel Flow (lb/s)	Time(min)	Fuel Burned in Segment (lbm)
Taxi Out	0	0.015	3000	0.3	0.256	15	230.4
Take Off	0-10000	0.38	18000	0.48	2.404	3.5	504.84
Climb	10000-35000	0.43	10000	0.47	1.306	11.5	901.14
Cruise	35000	0.8	5000	0.61	0.846	676.2	34323.912
Descend	35000-10000	0.38	10000	0.44	1.242	24.5	1825.74
Approach & Touchdown	10000-0	0.21	14000	0.38	1.498	8	719.04
Taxi In	0	0.015	3000	0.3	0.256	4	61.44
Total						742.7	38566.51

Table 8 Flight mission for designed engine 4

Segment	Altitude (ft)	Mach Number	Thrust (lbf)	TSFC (lbm/lbf*h)	Fuel Flow (lb/s)	Time(min)	Fuel Burned in Segment (lbm)
Taxi Out	0	0.015	3000	0.28	0.260	15	234
Take Off	0-10000	0.38	18000	0.39	2.13	3.5	447.3
Climb	10000-35000	0.43	10000	0.39	1.093	11.5	754.17
Cruise	35000	0.8	5000	0.546	0.826	676.2	33512.47
Descend	35000-10000	0.38	10000	0.34	1.105	24.5	1624.35
Approach & Touchdown	10000-0	0.21	14000	0.25	1.15	8	552
Taxi In	0	0.015	3000	0.28	0.260	4	62.4
Total						742.7	37186.69

According to the flight mission results CFM56-7B24 engine consumed the highest fuel with 41648lbm while the engines 1 and 2 had identical and the lowest fuel consumption during the mission. The fuel consumptions of geared engines 3 and 4 were higher than the non-geared engine of engine 1 and 2. Engine 4 carried out better fuel consumption with 37186.69 lbm than the engine 3 with 38566 lbm. Although ungeared engines showed better performance than the geared engines, we selected the engine 3 selected as our engine for hybrid propulsion system. Even though having 3.57% higher fuel consumption, the trade of reasons for selecting engine 3 instead of engine 4 were proper fan pressure ratio of 1.68 and lower mass flow rate which decreases the fan diameter, weight, and overall engine diameter. Additionally, engine 3 had 7.4% lower fuel consumption when compared to CFM56-7B24 engine. For these reasons, we selected and named the engine 3 as Century-250 in the project in light of the better performance results and reliability. The twin-spool turbofan engine with gear box selected whose station numbering, and engine configuration were shown in Fig. 4. As results of the parametric design studies, we decided to select engine 3 as our engine to carry out hybrid propulsion system.

5 DESIGN OF THE CENTURY-250 ENGINE

In this section, the design of the Century-250 engine was presented depending on parametric studies and optimizations. Then the component design was made, and performance results were compared with baseline engine CFM56-7B24. 0.8

Mach and 35.000ft is the standard design point for a passenger aircraft engine as they were selected for the cruise condition parameters. Turbofan engines are generally designed for takeoff conditions, so Century-250 engine is designed following this path. The Century-250 engine was designed as an ultra-high-bypass, twin-spool, axial turbofan engine. It consisted of 1 stage fan, 4 stage LPC, 4 stages HPC, 2 stage HPT, 4 stages LPT, and hot-cold nozzles. The geometry of Century-250 was shown in Fig. 6.

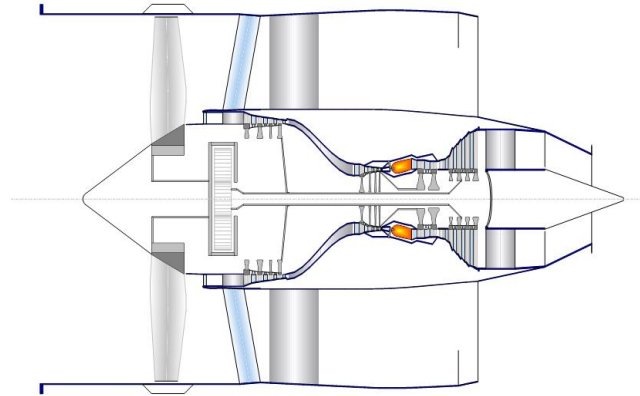


Figure 7 The Century-250 turbofan engine

5.1 PERFORMANCE CYCLE DESIGN AND ANALYSIS

Parametric cycle analyses of the reference engine were used in the preliminary design of the Century-250 engine. Our main design point was to provide electric power to flight and hybrid electric propulsion systems at 35.000ft and 0.8 Mach cruising conditions. Additionally, reducing fuel consumption, lowering engine weight, and reducing drag by decreasing the engine diameter were our main goals in the component designs. Before starting the design of the Century-250 engine, the requirements specified in the project request were noted and analyzed, and then the CFM56-7B24 engine was examined in the context of these requirements. The other engines presented in the project request, IAE V2500 and Pratt & Whitney PW1000G, were also analyzed in detail, with the four main parameters such as BPR, TIT, OPR, and SFC. On the other hand, it was aimed to achieve an ultra-high BPR value inspired by future technologies and to achieve this at high OPR values, as seen in similar engines. Thus, the design of the Century-250 engine was started with these goals and objectives and through GasTurb14 and AxStream software was used for this. In the design studies of the Century-250 engine, the BPR value was limited between 9 and 15, considering advanced technology. The other main parameter, OPR value, was found to be 26 in the CFM56-7B24 engine, 29.8 in the IAE V2500 engine [32], and 40 in Pratt & Whitney PW1000G engine [10]. In the studies conducted for the Century-250 engine, the OPR value was limited between 25 and 50.

The parametric section of the GasTurb14 software was used to find the best combination of the four main parameters of BPR, FPR, TIT, and OPR for reducing the specific fuel consumption (TSFC) of the Century-250 engine. Parametric studies were conducted to determine how TSFC value can be decreased. Fig. 7 shows the parametric study results evaluated by iterations. In Fig. 7 (a), optimum BPR, and TIT were searched for SFC and net thrust. Additionally, optimum OPR, FPR, and BPR were investigated for SFC in Fig. 7(b) whereas the optimum pressure ratio of HPC was searched against TIT, net thrust, and SFC (Fig. 7(c)). As a result of parametric and optimization studies, the BPR of 12 was found to be the most efficient value for the design. Moreover, the optimum OPR was found to be 39.58 with FPR, LPC, and HPC pressure ratios of 1.68 and 4, and 6, respectively. Besides T3 (HPC exit) and T4 (burner exit), temperatures were found to be 1607R and 3000R, respectively. All the parametric study results were given in Table 9 with the comparisons of baseline engine parameters and results. According to the results, the use of the Century-250 engine resulted in a 19.9% increase in the thrust of the CFM56-7B24 engine, while the specific fuel consumption (SFC)

of the baseline engine was decreased by 30.5% with the new engine at the takeoff condition. However, the thrust of Century-250 engine decreased by 2.9% when compared to baseline CFM56-7B24 engine.

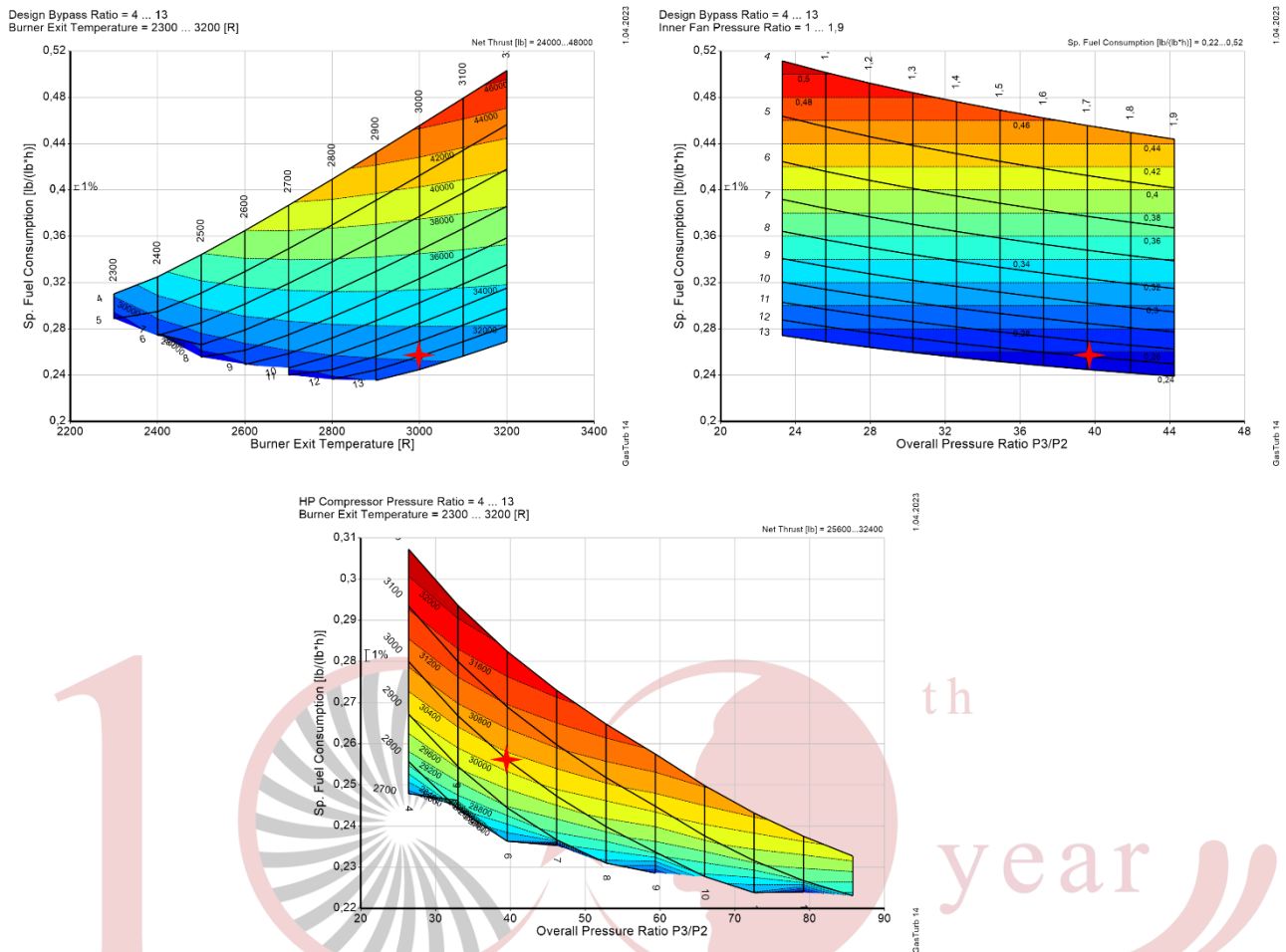


Figure 8 Parametric study results (a) BPR, TIT (T4) vs SFC, Thrust, (b) OPR vs SFC FPR, BPR (c) MFR vs SFC, BPR, OPR, Thrust

Table 9 shows the comparison of the baseline engine and the Century 250 design parameters and results of the cycle calculations.

Table 9 Baseline engine and the Century-250 design parameters and results

Mission	CFM56-7B24		CENTURY-250	
	Take-Off	Cruise	Take-Off	Cruise
Thrust (lb)	24227	5581	30268	5418
TSFC (lb/(lb*h))	0.36	0.68	0.25	0.62
Mass Flow (lb/s)	751	306	1338	515
T3(R)	1394	1323	1607	1389
T4(R)	2800	2805	3000	3000
V18/V8	0.57	0.53	0.43	0.37
BPR	5.3	5.21	12	12.14
OPR	26	29.95	39.58	38.9
FPR	1.4	1.4	1.68	1.66
LPC PR	1.81	1.86	4.0	3.93
HPC PR	10.57	11.66	6.0	6.15
LP Spool Speed	5173		3476	3439
IPC Spool Speed	-	-	10428	10316
HP Spool Speed	14461		23533	235357
Core Efficiency	0.45	0.51	0.49	0.57
Prop Efficiency	-	0.72	-	0.82

An increase in BPR also increased the mass flow rate of the engine from 751 lb/s to 1338 lb/s as well as cruise thrust increased from 306 lb/s to 674 lb/s. Furthermore, FPR of baseline engine increased from 1.4 to 1.68 with an OPR increase from 26 to 39.58. Optimized on design cycle of the Century-250 engine was illustrated in Fig. 8 (a). According to the on-design analyses, the rotational speed of HP, LP and IP spools were obtained as 23533 rpm, 3476 rpm, 10428 rpm, respectively.

Station	W lb/s	T R	P psia	WRstd lb/s	FN	Tsfc	WF	s NOX	Core Eff	Prop Eff	BPR	P2/P1	P3/P2	P5/P2	NGV Out. 2 Stage HPT	P16/P13	P16/P6	P16/P2	P6/P5	A8	XM18	XM8	WBld/w2	CD8	PWX	V18/v8_id	WBLD/w25	Wrec1/w25	Loading	WCHN/w25	WCHR/w25	WCLN/w25	WCLR/w25	WBLD/w25	Gear Rat	WlkBy/w25	wkLP/w25	hum [%]	war0	FHV	Fuel		
amb																																											
2	1338,479	518,67	14,696	1352,000		30268,34			0,4983	0,0000	12,0000	0,9900	39,58	1,7003	2 Stage HPT	0,9800	0,78051	1,27400	0,96000	339,15	3804,10	0,87041	0,00000	0,97262	200,0	0,43487	0,00000	0,00000	100,00	0,06500	0,02500	0,01667	0,00333	0,00000	3,00000	0,00000			0,0	0,00000	18552,4	Generic	
13	1235,520	563,48	18,914	1000,610		0,2561	2,15304	1,7824	0,4983	0,0000	12,0000	0,9900	39,58	1,7003	2 Stage HPT	0,9800	0,78051	1,27400	0,96000	339,15	3804,10	0,87041	0,00000	0,97262	200,0	0,43487	0,00000	0,00000	100,00	0,06500	0,02500	0,01667	0,00333	0,00000	3,00000	0,00000			0,0	0,00000	18552,4	Generic	
21	102,960	612,79	24,733	66,496					0,4983	0,0000	12,0000	0,9900	39,58	1,7003	2 Stage HPT	0,9800	0,78051	1,27400	0,96000	339,15	3804,10	0,87041	0,00000	0,97262	200,0	0,43487	0,00000	0,00000	100,00	0,06500	0,02500	0,01667	0,00333	0,00000	3,00000	0,00000			0,0	0,00000	18552,4	Generic	
22	102,960	612,79	24,486	67,167					0,4983	0,0000	12,0000	0,9900	39,58	1,7003	2 Stage HPT	0,9800	0,78051	1,27400	0,96000	339,15	3804,10	0,87041	0,00000	0,97262	200,0	0,43487	0,00000	0,00000	100,00	0,06500	0,02500	0,01667	0,00333	0,00000	3,00000	0,00000			0,0	0,00000	18552,4	Generic	
24	102,960	945,79	97,944	20,861					0,4983	0,0000	12,0000	0,9900	39,58	1,7003	2 Stage HPT	0,9800	0,78051	1,27400	0,96000	339,15	3804,10	0,87041	0,00000	0,97262	200,0	0,43487	0,00000	0,00000	100,00	0,06500	0,02500	0,01667	0,00333	0,00000	3,00000	0,00000			0,0	0,00000	18552,4	Generic	
25	102,960	945,79	95,985	21,287					0,4983	0,0000	12,0000	0,9900	39,58	1,7003	2 Stage HPT	0,9800	0,78051	1,27400	0,96000	339,15	3804,10	0,87041	0,00000	0,97262	200,0	0,43487	0,00000	0,00000	100,00	0,06500	0,02500	0,01667	0,00333	0,00000	3,00000	0,00000			0,0	0,00000	18552,4	Generic	
3	100,901	1607,23	575,910	4,532					0,4983	0,0000	12,0000	0,9900	39,58	1,7003	2 Stage HPT	0,9800	0,78051	1,27400	0,96000	339,15	3804,10	0,87041	0,00000	0,97262	200,0	0,43487	0,00000	0,00000	100,00	0,06500	0,02500	0,01667	0,00333	0,00000	3,00000	0,00000			0,0	0,00000	18552,4	Generic	
31	91,634	1607,23	575,910	5,996					0,4983	0,0000	12,0000	0,9900	39,58	1,7003	2 Stage HPT	0,9800	0,78051	1,27400	0,96000	339,15	3804,10	0,87041	0,00000	0,97262	200,0	0,43487	0,00000	0,00000	100,00	0,06500	0,02500	0,01667	0,00333	0,00000	3,00000	0,00000			0,0	0,00000	18552,4	Generic	
4	93,787	3000,00	552,873	5,996					0,4983	0,0000	12,0000	0,9900	39,58	1,7003	2 Stage HPT	0,9800	0,78051	1,27400	0,96000	339,15	3804,10	0,87041	0,00000	0,97262	200,0	0,43487	0,00000	0,00000	100,00	0,06500	0,02500	0,01667	0,00333	0,00000	3,00000	0,00000			0,0	0,00000	18552,4	Generic	
405	97,906	2945,87	552,873	6,331					0,4983	0,0000	12,0000	0,9900	39,58	1,7003	2 Stage HPT	0,9800	0,78051	1,27400	0,96000	339,15	3804,10	0,87041	0,00000	0,97262	200,0	0,43487	0,00000	0,00000	100,00	0,06500	0,02500	0,01667	0,00333	0,00000	3,00000	0,00000			0,0	0,00000	18552,4	Generic	
41	100,480	2914,20	552,873	6,331					0,4983	0,0000	12,0000	0,9900	39,58	1,7003	2 Stage HPT	0,9800	0,78051	1,27400	0,96000	339,15	3804,10	0,87041	0,00000	0,97262	200,0	0,43487	0,00000	0,00000	100,00	0,06500	0,02500	0,01667	0,00333	0,00000	3,00000	0,00000			0,0	0,00000	18552,4	Generic	
43	100,480	2326,10	187,548						0,4983	0,0000	12,0000	0,9900	39,58	1,7003	2 Stage HPT	0,9800	0,78051	1,27400	0,96000	339,15	3804,10	0,87041	0,00000	0,97262	200,0	0,43487	0,00000	0,00000	100,00	0,06500	0,02500	0,01667	0,00333	0,00000	3,00000	0,00000			0,0	0,00000	18552,4	Generic	
44	103,054	2309,18	187,548						0,4983	0,0000	12,0000	0,9900	39,58	1,7003	2 Stage HPT	0,9800	0,78051	1,27400	0,96000	339,15	3804,10	0,87041	0,00000	0,97262	200,0	0,43487	0,00000	0,00000	100,00	0,06500	0,02500	0,01667	0,00333	0,00000	3,00000	0,00000			0,0	0,00000	18552,4	Generic	
45	104,770	2294,53	183,797	17,620					0,4983	0,0000	12,0000	0,9900	39,58	1,7003	2 Stage HPT	0,9800	0,78051	1,27400	0,96000	339,15	3804,10	0,87041	0,00000	0,97262	200,0	0,43487	0,00000	0,00000	100,00	0,06500	0,02500	0,01667	0,00333	0,00000	3,00000	0,00000			0,0	0,00000	18552,4	Generic	
49	104,770	1481,46	24,737						0,4983	0,0000	12,0000	0,9900	39,58	1,7003	2 Stage HPT	0,9800	0,78051	1,27400	0,96000	339,15	3804,10	0,87041	0,00000	0,97262	200,0	0,43487	0,00000	0,00000	100,00	0,06500	0,02500	0,01667	0,00333	0,00000	3,00000	0,00000			0,0	0,00000	18552,4	Generic	
5	105,113	1481,25	24,737	105,529					0,4983	0,0000	12,0000	0,9900	39,58	1,7003	2 Stage HPT	0,9800	0,78051	1,27400	0,96000	339,15	3804,10	0,87041	0,00000	0,97262	200,0	0,43487	0,00000	0,00000	100,00	0,06500	0,02500	0,01667	0,00333	0,00000	3,00000	0,00000			0,0	0,00000	18552,4	Generic	
8	105,113	1481,25	23,748	109,926					0,4983	0,0000	12,0000	0,9900	39,58	1,7003	2 Stage HPT	0,9800	0,78051	1,27400	0,96000	339,15	3804,10	0,87041	0,00000	0,97262	200,0	0,43487	0,00000	0,00000	100,00	0,06500	0,02500	0,01667	0,00333	0,00000	3,00000	0,00000			0,0	0,00000	18552,4	Generic	
18	1235,520	563,48	18,535	1021,031					0,4983	0,0000	12,0000	0,9900	39,58	1,7003	2 Stage HPT	0,9800	0,78051	1,27400	0,96000	339,15	3804,10	0,87041	0,00000	0,97262	200,0	0,43487	0,00000	0,00000	100,00	0,06500	0,02500	0,01667	0,00333	0,00000	3,00000	0,00000			0,0	0,00000	18552,4	Generic	
Bleed	0,000	1607,23	575,909						0,4983	0,0000	12,0000	0,9900	39,58	1,7003	2 Stage HPT	0,9800	0,78051	1,27400	0,96000	339,15	3804,10	0,87041	0,00000	0,97262	200,0	0,43487	0,00000	0,00000	100,00	0,06500	0,02500	0,01667	0,00333	0,00000	3,00000	0,00000			0,0	0,00000	18552,4	Generic	
Efficiency	isent	polytr	RNI	P/P					0,4983	0,0000	12,0000	0,9900	39,58	1,7003	2 Stage HPT	0,9800	0,78051	1,27400	0,96000	339,15	3804,10	0,87041	0,00000	0,97262	200,0	0,43487	0,00000	0,00000	100,00	0,06500	0,02500	0,01667	0,00333	0,00000	3,00000	0,00000			0,0	0,00000	18552,4	Generic	
Outer LPC	0,9000	0,9037	0,990	1,300					0,4983	0,0000	12,0000	0,9900	39,58	1,7003	2 Stage HPT	0,9800	0,78051	1,27400	0,96000	339,15	3804,10	0,87041	0,00000	0,97262	200,0	0,43487	0,00000	0,00000	100,00	0,06500	0,02500	0,01667	0,00333	0,00000	3,00000	0,00000			0,0	0,00000	18552,4	Generic	
Inner LPC	0,9000	0,9072	0,990	1,700					0,4983	0,0000	12,0000	0,9900	39,58	1,7003	2 Stage HPT	0,9800	0,78051	1,27400	0,96000	339,15	3804,10	0,87041	0,00000	0,97262	200,0	0,43487	0,00000	0,00000	100,00	0,06500	0,02500	0,01667	0,00333	0,00000	3,00000	0,00000			0,0	0,00000	18552,4	Generic	
IP Compressor	0,8800	0,9005	1,367	4,000					0,4983	0,0000	12,0000	0,9900	39,58	1,7003	2 Stage HPT	0,9800	0,78051	1,27400	0,96000	339,15	3804,10	0,87041	0,00000	0,97262	200,0	0,43487	0,00000	0,00000	100,00	0,06500	0,02500	0,01667	0,00333	0,00000	3,00000	0,00000			0,0	0,00000	18552,4	Generic	
HP Compressor	0,8800	0,9042	3,192	6,000					0,4983	0,0000	12,0000	0,9900	39,58	1,7003	2 Stage HPT	0,9800	0,78051	1,27400	0,96000	339,15	3804,10	0,87041	0,00000	0,97262	200,0	0,43487	0,00000	0,00000	100,00	0,06500													

	Units	St 2	St 22	St 24	St 25	St 3	St 4	St 44	St 45	St 5	St 6	St 8	St 13	St 16	St 18
Mass Flow	lb/s	1338.48	102.96	102.96	102.96	100.901	93,7874	103,054	104,77	105,113	105,113	105,113	1235,52	1235,52	1235,52
Total Temperature	R	518,67	612,788	945,786	945,786	1607,23	3000	2309,18	2294,53	1481,25	1481,25	1481,25	563,48	563,48	563,48
Static Temperature	R	478,194	583,737	917,708	910,517	1589,94	2995,66	2252,23	1421,03	1432,28	1310,47	531,408	536,73	527,382	527,382
Total Pressure	psia	14,549	24,4859	97,9438	95,9849	575,91	552,873	187,548	183,797	24,7372	23,7477	23,7477	18,9137	18,5354	18,5354
Static Pressure	psia	10,9521	20,6464	87,8182	83,645	552,306	549,319	159,76	169,785	20,9898	20,7789	14,6963	15,3998	15,6267	14,696
Velocity	ft/s	696,891	591,941	590,946	662,307	479,121	257,575	1117,29	766,89	904,563	817,135	1515,91	621,532	567,643	659,244
Area	in ²	4474,06	262,369	97,1383	90,283	32,3445	105,938	68,5015	94,2279	419,71	473,057	329,87	3659,73	3987,13	3588,24
Mach Number		0,649999	0,5	0,4	0,45	0,25	0,1	0,5	0,35	0,5	0,5	0,87039	0,55	0,5	0,585588
Density	lb/ft ³	0,061817	0,095464	0,258281	0,249751	0,937588	0,494938	0,193892	0,203472	0,039868	0,039157	0,030269	0,078217	0,078582	0,075212
Spec Heat @ T	BTU/(lb·R)	0,240085	0,240994	0,247364	0,247364	0,267525	0,306155	0,29393	0,293452	0,271845	0,271845	0,271845	0,240424	0,240424	0,240424
Spec Heat @ Ts	BTU/(lb·R)	0,239956	0,240658	0,246562	0,246357	0,267015	0,306098	0,292166	0,292578	0,269853	0,270242	0,266026	0,240126	0,240143	0,240113
Enthalpy @ T	BTU/lb	-4,31603	18,343	99,488	99,488	269,698	686,841	477,489	472,971	242,318	242,318	242,318	6,45803	6,45803	6,45803
Enthalpy @ Ts	BTU/lb	-14,0214	11,3407	92,5093	90,722	265,111	685,515	452,543	460,597	225,966	228,975	196,395	-1,26181	0,014292	-2,22703
Entropy Function @ T		-0,11924	0,465683	2,00516	2,00516	3,98682	6,75723	5,59451	5,56485	3,7608	3,7608	3,7608	0,171092	0,171092	0,171092
Entropy Function @ Ts		-0,40323	0,295124	1,89603	1,86755	3,94497	6,75078	5,43415	5,48556	3,59653	3,62726	3,28091	-0,034442	3,8816E-4	-0,061019
Exergy	BTU/lb	-0,357833	20,0117	95,7058	94,9869	258,44	575,55	369,102	364,92	127,099	125,646	125,646	9,4212	8,70231	8,70231
Gas Constant	BTU/(lb·R)	0,068607	0,068607	0,068607	0,068607	0,068607	0,068606	0,068606	0,068606	0,068606	0,068606	0,068606	0,068607	0,068607	0,068607
Fuel-Air-Ratio		0	0	0	0	0	0	0,023496	0,020911	0,020911	0,020911	0	0	0	0
Water-Air-Ratio		0	0	0	0	0	0	0	0	0	0	0	0	0	0
Inner Radius	in	11,868	14,9441	14,4557	5,11038	5,11805	7,74353	7,74353	7,74353	8,13071	8,13071	4,01571	18,4374	14,8059	14,8341
Outer Radius	in	39,5599	17,5168	15,4865	7,40635	6,05025	9,67902	9,04251	9,48451	14,1318	14,7203	11,1392	38,7926	38,5792	37,8277
Axial Position	in	19,78	19,78	45,8393	57,0769	73,7498	80,3581	87,014	87,7729	101,308	114,733	127,397	43,2058	97,4767	101,25

(a)

	Units	St 2	St 22	St 24	St 25	St 3	St 4	St 44	St 45	St 5	St 6	St 8	St 13	St 16	St 18
Mass Flow	lb/s	515,804	39,2269	39,2268	39,2268	38,4422	35,8512	39,3816	39,97	40,1662	40,1662	40,1662	476,577	476,577	476,577
Total Temperature	R	444,378	524,01	805,832	805,832	1389,38	2999,88	2368,07	2351,92	1673,45	1673,45	1673,45	482,172	482,172	482,172
Static Temperature	R	410,375	499,598	781,074	774,706	1374,07	2995,58	2281,59	2309,01	1607,77	1620,07	1434,49	454,625	459,178	401,677
Total Pressure	psia	5,21998	8,70068	34,2117	33,5206	203,059	194,974	76,5677	75,0354	15,2622	14,6519	14,6519	6,74872	6,61377	6,61377
Static Pressure	psia	3,95216	7,36443	30,6181	29,1387	194,716	193,723	65,2388	69,3247	12,9683	12,8355	7,88812	5,49446	5,57544	3,49298
Velocity	ft/s	638,738	541,203	549,824	616,493	446,163	257,373	1130,61	795,94	957,913	865,205	1815,89	574,91	525,253	982,761
Area	in ²	4473,6	262,335	97,1009	90,2548	32,4393	114,918	64,9917	89,2349	277,344	312,614	214,604	3659,41	3986,72	2975,2
Mach Number		0,642984	0,493884	0,402426	0,453024	0,249338	0,10001	0,500217	0,350125	0,499992	0,449995	1	0,549914	0,499925	0,999923
Density	lb/ft ³	0,025994	0,039786	0,105803	0,101519	0,382478	0,17455	0,077177	0,081037	0,021771	0,021384	0,014842	0,03262	0,032773	0,023471
Spec Heat @ T	BTU/(lb·R)	0,239848	0,240102	0,244056	0,244056	0,260996	0,308053	0,296622	0,296139	0,279164	0,279164	0,279164	0,239969	0,239969	0,239969
Spec Heat @ Ts	BTU/(lb·R)	0,23974	0,240024	0,24353	0,243395	0,260512	0,307993	0,294871	0,295267	0,277164	0,277567	0,2771465	0,239881	0,239895	0,239712
Enthalpy @ T	BTU/lb	-22,1298	-3,0357	65,1295	65,1295	212,183	690,272	496,939	491,881	296,283	296,283	296,283	-13,0675	-13,0675	-13,0675
Enthalpy @ Ts	BTU/lb	-30,2829	-8,88901	59,0882	57,5343	208,205	688,948	471,394	479,221	277,945	281,323	230,386	-19,6727	-18,5809	-32,3684
Entropy Function @ T		-0,659571	0,083442	1,43243	1,43243	3,42631	6,78814	5,72516	5,69278	4,26495	4,26495	4,26495	-0,374275	-0,374275	-0,374275
Entropy Function @ Ts		-0,937802	-0,250182	1,32146	1,29234	3,38435	6,7817	5,56504	5,61362	4,10207	4,13258	3,64573	-0,579888	-0,545058	-1,01268
Exergy	BTU/lb	11,8428	29,1745	93,3755	92,8241	234,675	620,847	430,979	426,249	226,199	225,096	225,096	20,1366	19,5909	19,5909
Gas Constant	BTU/(lb·R)	0,068607	0,068607	0,068607	0,068607	0,068607	0,068606	0,068606	0,068606	0,068606	0,068606	0,068606	0,068607	0,068607	0,068607
Fuel-Air-Ratio		0	0	0	0	0	0	0,026909	0,024437	0,024069	0,023948	0,023948	0	0	0
Water-Air-Ratio		0	0	0	0	0	0	0	0	0	0	0	0	0	0

(b)

Figure 10 Thermodynamic, kinetic, and geometric results of the stations (a) takeoff condition (b) cruise condition

6 ENGINE COMPONENT DESIGN

Engine component design was started with an air compression unit that consists of a fan, low-pressure compressor, and high-pressure compressors. These components also provide the overall pressure ratio (OPR) of the engine. Axial compressors were used due to higher levels of mass flow rate capacity and pressures.

6.1 FAN DESIGN

Single stage axial fan was used in the Century-250 engine and design parameters were provided from GasTurb14 for the AxStream software in which fan design was performed (see Table 10). Design parameters were shown in Table 5. FPR was selected as 1.52 for a fan and the FPR has been reported to be in the range of 1.4 and 1.6 [17]. Inlet total pressure and temperature were 14.5 psi and 522 R, respectively. The outlet's total pressure and temperature were 21.82 psi and 958.6R, respectively. Additionally, MRF and rotational speed were found to be 958.6 lb/s and 4717 rpm, respectively. Moreover, fan tip and hub diameters were obtained as 67.68 and 25.24 inches, respectively.

Table 10 GasTurb14 data for fan design boundary conditions and geometric parameters

Fan Design			
Total Pressure <i>(inlet)</i> [psi]	14.54	Shaft Rotational Speed [RPM]	3476
Total Pressure <i>(outlet)</i> [psi]	24.48	Tip Diameter [inch]	79.12
Pressure Ratio	1.68	Hub Diameter [inch]	27.9
Total Temperature <i>(inlet)</i> [R]	518.67	Hub to Tip Ratio	0.35
Total Temperature <i>(outlet)</i> [R]	612.78	Blade Height [inch]	25.6
Mass Flow [lb/s]	1338.48	Number of Stage	1

The preliminary design was done in AxStream using 5000 iterations with the parameter given in Table 5. After the 1D calculations, 2D streamline calculations were performed to optimize the flow path of the fan. The 2D calculations were done to find the inlet total pressure for a given mass flow rate with 500 iterations. The relative Mach number, total pressure, and temperatures were evaluated and compared to Gasturb14 and literature findings (see Fig. 5).

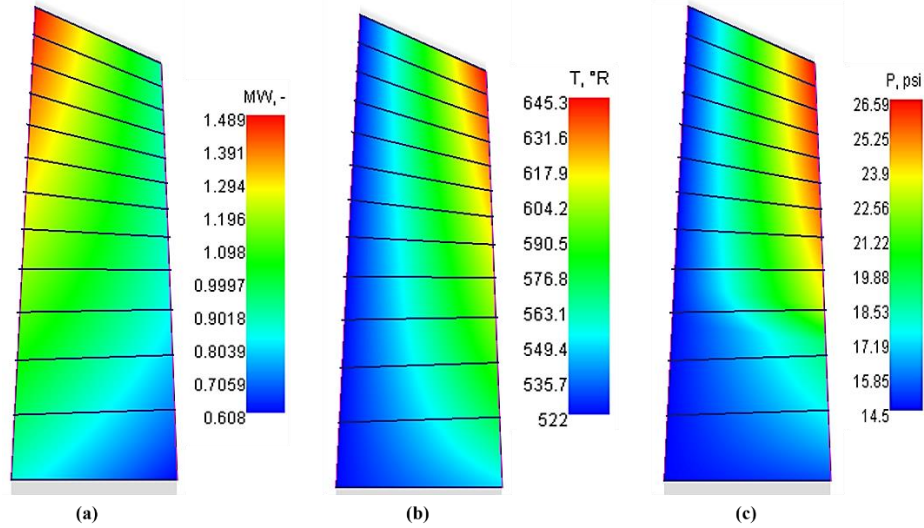


Figure 11 Axial fan 2D streamline calculation result (a) relative Mach number, (b) Total temperature, (c) Total pressure

According to the 2D streamline calculations, the fan rotor blade tip relative Mach number was obtained as 1.48 which shouldn't exceed 1.5 (see Fig. 10 (a)). Fig. 10 (b) and (c) show the total temperature and pressure deviation in fan rotor blades where the 522R inlet temperature raised to 645.3R after the compression process. Additionally, the inlet pressure of 14.5 psi was increased to 26.59 psi in the fan rotor blades. The AxStream fan design results are illustrated in Table 5. It was observed that de Haller number of the fan was 0.86 which should be larger than 0.72 for lower loss and higher diffusion in the fan blades [8]. In addition, work and flow coefficients were found to be 0.94 and 1.18 which were consistent with the literature [3]. A good polyprotic efficiency of 87% was achieved at the end of the design process.

Table 5 Fan design results

Parameter	STAGE 1
Work Coefficient	0.94
Flow Coefficient	1.18
Stage Pressure Ratio	1.78
Number of Blades	22
Aspect Ratio	2.54
Blade Chord [inch]	9.71
Solidity	1.24
Stagger Angle [tan.deg]	21.27
Leading Edge Radius [inch]	0.09
Trailing Edge Radius [inch]	0.09
De-Haller Number	0.86
Polytropic Efficiency [$\eta_{polytropic}$]	0.87
Degree of Reaction at Hub	1

6.1.1 OFF-DESIGN ANALYSIS OF FAN

Off design of fan was performed by using GasTurb14 and a comparison of the on and off design performances of the axial fan were illustrated in the maps (see Fig. 11). According to the on-design analysis fan isentropic efficiency was found to be 0.93 while it was 0.88 for cruise conditions. The performance map showed that fan was far from the surge and choke margin (see the red line and blue-orange dots on the map). The calculated surge margins of on and off designs were also shown in Fig.11 where the fan surge margin was %30 and %25 at on-off design conditions, respectively. Design results showed that the fan could operate safely during takeoff and cruise conditions.

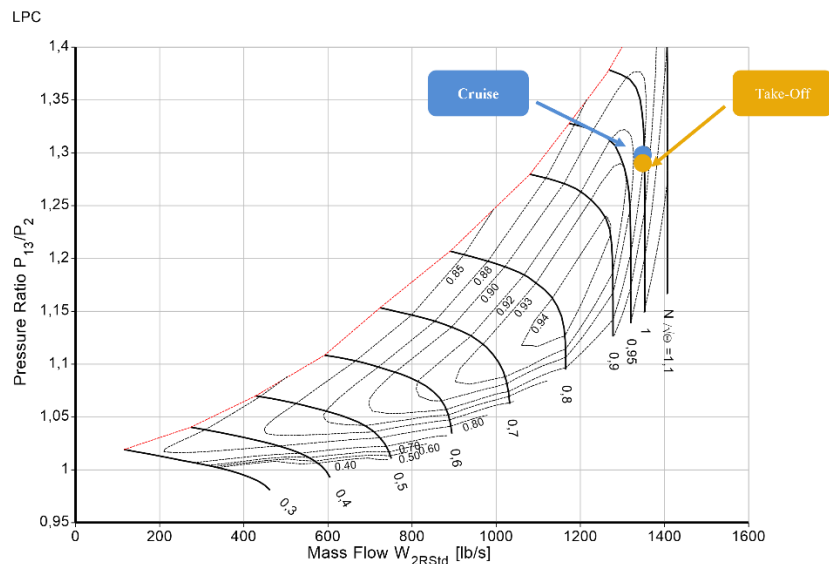


Figure 12 On and off design performance of the fan

6.1.2 FAN BLADE MATERIALS

Using composite materials as a fan blade is a good innovation and carbon fiber is one of the greatest applications whose density is lower than three times titanium alloys [Kosmatka, 2009]. Thus, large fan weight can be decreased using Carbon Fiber Reinforced Plastic composite (CFPR) as blade and fan case material. The density of the carbon fiber is 0.06 lb/in^3 , Young's modulus and tensile stress are 37709 ksi and 507-725 MPa, respectively [Pandita, 2014]. Leading edge blade material was chosen as Ti6AlV4 alloys in the fan.



Figure 13 3-D CAD drawing of the fan

6.2 COMPRESSORS DESIGN

Axial and radial flow compressors are used in aviation engines. The axial compressors are selected when the higher-pressure ratios and mass flow rates required. In the Century 250 engine we designed 2 stages LPC and 10 stages HPC through the AxStream. Typical axial compressor design parameters were given in Table 7[19,36]. These parameters were taken consideration and results were compared to these parameters in the axial compressor designs.

Table 6 Typical axial compressor design parameters used in the literature

PARAMETER	Range of Values	Parameter	Range of Values
Flow Coefficient	$0.3 \leq \phi \leq 0.9$	Tip Rotational Speed	$1480 \leq \omega r_t \leq 1640$ ft/s
HPC Max. Exit Temperature [R]	1700-1800	Hub/Tip Ratio at Inlet	0.6-0.75
Axial Mach Number	$0.3 \leq M_z \leq 0.6$	De Haller Number	$W_2 / W_1 \geq 0.72$
HPC Pressure Ratio	$\Pi_c < 20$	Degree of Reaction at Hub	$0.15 \leq A$
Reynolds Number Based on Chord	$300,000 \leq Re_c$	LPC Pressure Ratio	1 Stage: $1.5 \leq PR \leq 2$ 2 Stage: $2 \leq PR \leq 3.5$ 3 Stage: $3.5 \leq PR \leq 4.5$
DCA Blade (Range)	$0.8 \leq M \leq 1.2$	Aspect Ratio Fan	$2 \leq AR \leq 5$
Loading Coefficient	$0.2 \leq \psi \leq 0.5$	Aspect Ratio Compressor	$1.0 \leq AR \leq 4.0$
Hub Rotational Speed	$\omega r_h \leq 1250$ ft/s	Taper Ratio	$0.8 \leq TR \leq 1$
Solidity	$1.0 \leq \sigma \leq 2.0$	Axial Gap Between Blade Rows	$0.23c_z - 0.25c_z$
Tip Relative Mach Number	$(M_{1r})_{tip} \leq 1.7$	Pressure Ratio for One Stage	$1.5 \leq PR \leq 2.0$
Polytropic Efficiency	$0.88 \leq e_c \leq 0.92$	D-Factor	$0.5 \leq D \leq 0.6$

6.2.1 LOW PRESSURE COMPRESSOR (LPC) DESIGN

In the LPC design of the Century 250 engine, geometric data and boundary conditions were obtained from GasTurb14 and entered the AxStream (see Table 8). The air mass flow rate of the LPC was 59.96 lb/s and the stage number was 2 with the pressure ratio of 1.68. The total inlet temperature and pressures were found to be 592.6R and 21.8 psi, respectively.

Table 7 Geometric and boundary layer parameters of the LPC

Thermodynamic and Geometrical Properties			
Total Pressure (inlet) [psi]	24.48	Shaft Rotational Speed [RPM]	10428
Total Pressure (outlet) [psi]	97.94	1 st Stage Tip Diameter [inch]	36.61
Pressure Ratio	1.68	4 th Stage Tip Diameter [inch]	34.04
Total Temperature (inlet) [R]	612.78	1 st Stage Hub Diameter [inch]	32.35
Total Temperature (outlet) [R]	945.78	4 th Stage Hub Diameter [inch]	32.45
Mass Flow [lb/s]	102.96	1 st Stage Blade Height [inch]	2.13
Number Of Stage	4	4 th Stage Blade Height [inch]	0.79

There are three main flow annulus design which are constant tip, constant hub and mean line designs. To achieve the best compressor results and annulus area, mean line design was selected in the LPC design. After preliminary design in AxStream flow path optimize and revised via 2D streamline calculations by using 11 streamlines. Find outlet pressure for given mass flow rate boundary layer was used with 500 iterations in the AxStream design to achieve targeted polytropic efficiency. DCA blade profiles selected for LPC, and flow path optimized according to this type blading. The average polytropic efficiency was 87.5 for LPC after the optimizations. Fig. 7 shows relative Mach number, total temperature, and pressure changes through the annulus of LPC according to the 2D streamline calculations. It was observed that relative tip number at the inlet rotor tip was 1.18 and outlet Mach number was obtained as 0.5 which was consistent with the literature. Inlet total temperature was found to be 685R and the exit was 997R which were consistent with the GasTurb14 results. The total pressure ratio was calculated as 3.24 with the inlet and exit total pressures of 33.89 and 109.9 psi, respectively. The AxStream design results were shown in Table 8. De Haller numbers were not

lower than 0.72[24]. Furthermore, work and flow coefficients (loading factor) were found in range of values given in Table 7, respectively.

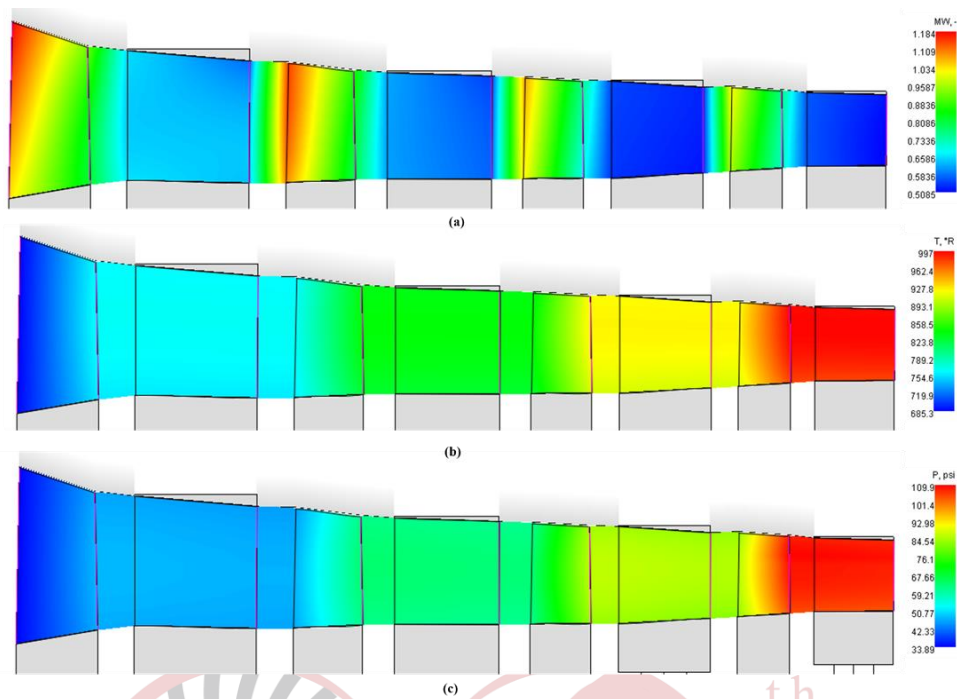


Figure 14 2D Streamline calculation results of the LPC, (a) Relative Mach number, (b) Total temperature, (c) Total pressure

Table 8 AxStream design results of the LPC

Parameter	STAGE 1		STAGE 4	
	Rotor	Stator	Rotor	Stator
Work Coefficient	0.33		0.3	
Flow Coefficient	0.63		0.6	
Stage Pressure Ratio	1.37		1.26	
Polytropic Efficiency [η polytropic]	0.84		0.88	
Degree of Reaction at Hub	1.05		0.92	
Number of Blades	30	30	46	46
Aspect Ratio	1.43	1.05	1.04	0.91
Blade Chord [inch]	1.62	1.62	1.06	1.06
Solidity	0.57	0.57	0.58	0.58
De-Haller Number	0.81	0.98	0.77	0.91

6.2.1.1 OFF-DESIGN ANALYSIS OF LPC

The comparison of the on and off design performance can be seen in Fig. 8. The isentropic efficiency was 0.83 at the takeoff and it was 0.88 for the cruise condition. Moreover, design points were not closer to surge or choke regions.

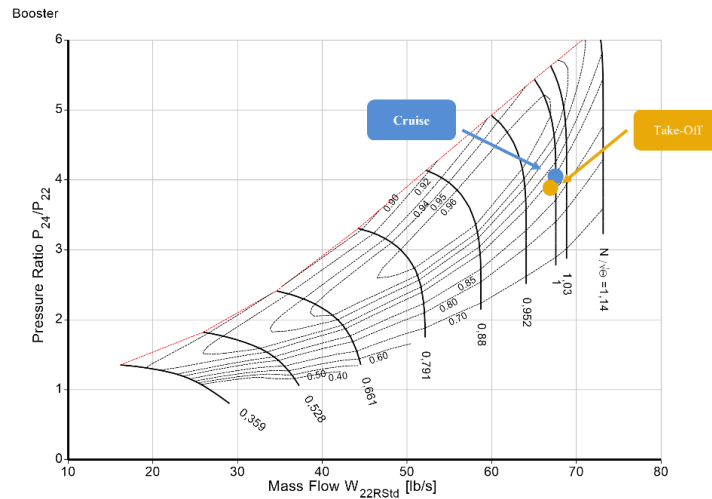


Figure 15 Performance map of the LPC at the cruise and take off conditions

6.2.1.2 LPC MATERIAL

LPC blade and disk material was selected Ti6242 alloys which have the density of 0.164 lb/m^3 , Young's modulus of 16500 ksi and a tensile stress of 101 ksi.



Figure 16 3-D CAD drawing of the LPC

6.2.2 HIGH PRESSURE COMPRESSOR (HPC) DESIGN

The boundary conditions and geometric data evaluated from the GasTurb14 for AxStream was shown in Table 9.

Table 9 Boundary condition and geometric data used in HPC design

Thermodynamic and Geometrical Properties			
Total Pressure $(inlet)$ [psi]	95.98	Shaft Rotational Speed [RPM]	20755
Total Pressure $(outlet)$ [psi]	575.91	1 st Stage Tip Diameter [inch]	14.55
Pressure Ratio	6	4 th Stage Tip Diameter [inch]	13.25
Total Temperature $(inlet)$ [R]	945.78	1 st Stage Hub Diameter [inch]	10.77
Total Temperature $(outlet)$ [R]	1607.23	4 th Stage Hub Diameter [inch]	12.19
Mass Flow [lb/s]	102.96	1 st Stage Blade Height [inch]	1.9
Number Of Stage	4	4 th Stage Blade Height [inch]	0.53

HPC was designed as 4 stages and annulus of the HPC was optimized according to efficiency, inlet/ outlet temperatures and pressures via streamline calculations. Similar to LPC DCA blade profile was selected for HPC and

2D streamline calculations were done using 9 streamlines. Fig. 9 shows relative Mach number, total temperature, and pressure changes through the annulus of HPC. When looking at the relative Mach numbers, it was detected that tip Mach number was 0.9 and it did not exceed the 1.5. At the exit of the HPC it decreased to 0.28 which presented good speed before the diffuser. Inlet total temperature was 997R, whereas it was 1688

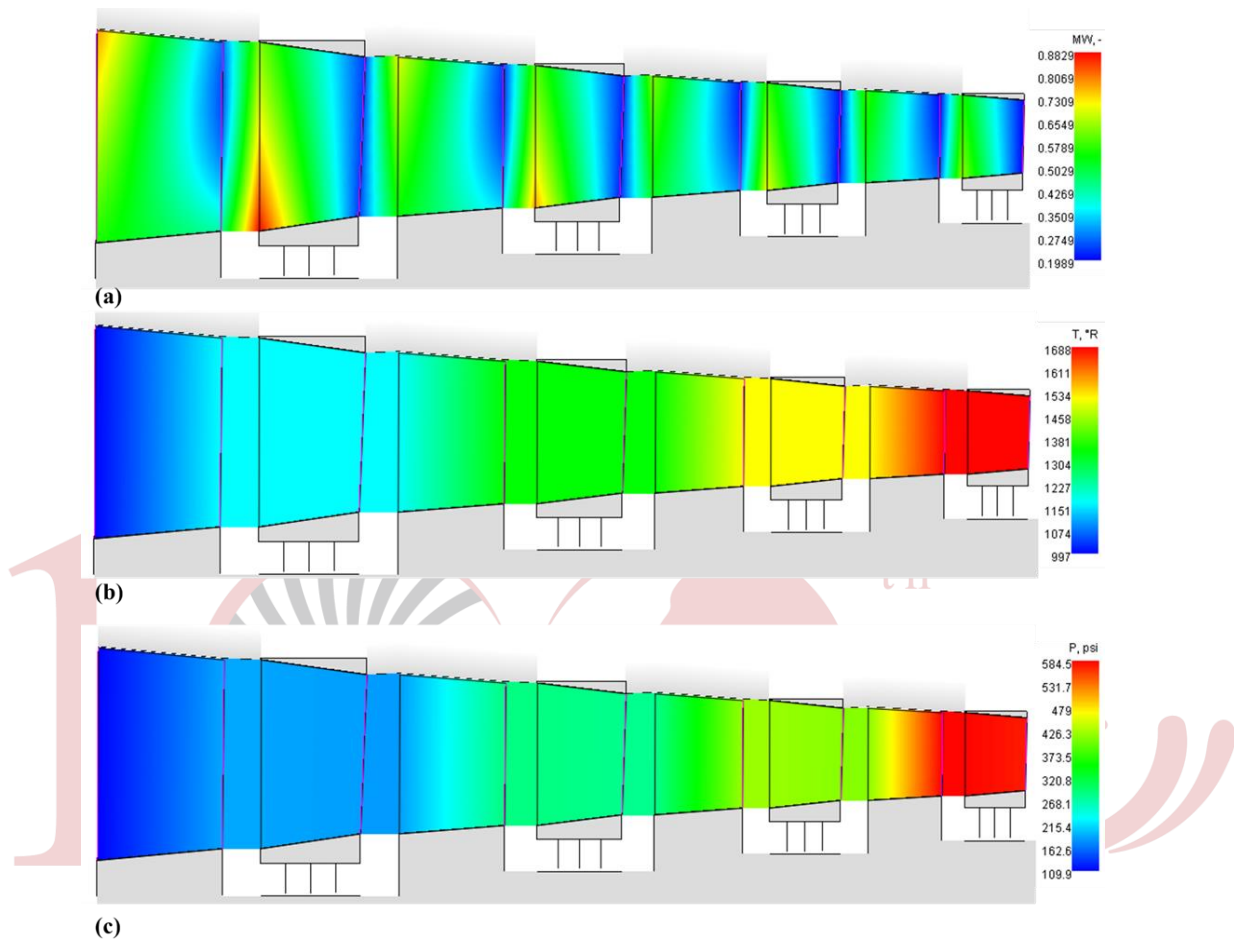


Figure 17 2D Streamline calculation results of the HPC (a) Relative Mach, (b) Total Temperature and (c) Total Pressure

The total temperature at the HPC inlet was 997R and increased to 1680K at the HPC exit. Moreover, total inlet pressure was found to be 109.9 psi whereas it decreased to 584.5 psi at the HPC exit. The design results of the HPC were shown in Table 10. The first and the last stages work coefficients were 1.05 and 0.4. In addition, flow coefficients were found to be 0.73 and 1.07 for the first and last stages. The stage pressure ratio was 1.92 at the first stage and it decreases to 1.03 at the last stage. The findings were consistent with the reported literature specifications.

Table 10 Design results of the HPC

Parameter	STAGE 1		STAGE 4	
	Rotor	Stator	Rotor	Stator
Work Coefficient	1.05		0.4	
Flow Coefficient	0.73		1.07	
Stage Pressure Ratio	1.91		1.03	
Polytropic Efficiency [η polytropic]	0.82		0.78	
Degree of Reaction at Hub	0.39		0.8	
Number of Blades	62	70	91	96
Aspect Ratio	1.9	1.41	1.07	1.02
Blade Chord [inch]	1.16	1.02	0.63	0.6
Solidity	1.9	1.9	1.61	1.6
De-Haller Number	0.72	0.68	0.87	0.95

6.2.2.1 OFF-DESIGN PERFORMANCE OF HPC

The performance map of HPC showed that HPC can operate safely not only at cruise condition but also at takeoff condition. Furthermore, isentropic efficiencies of cruise and takeoff conditions were 0.88 (see Fig. 17).

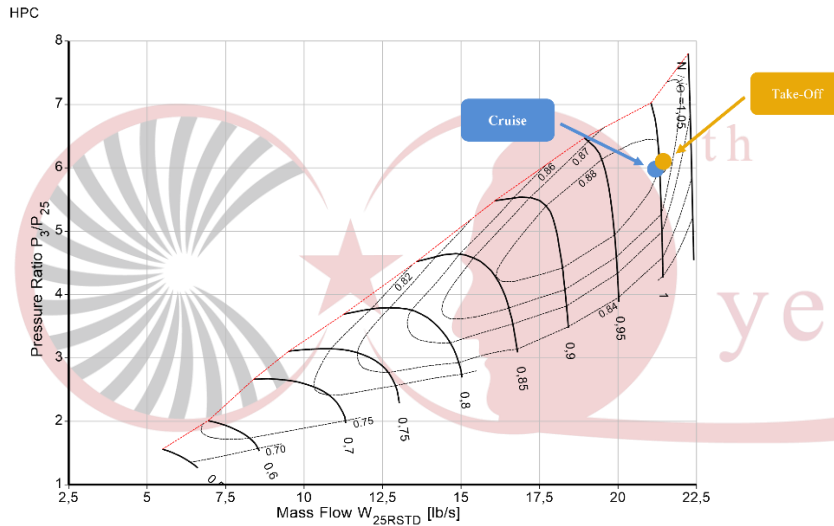


Figure 18 Performance map of HPC at cruise and take off conditions

According to the performance map, it can be observed that HPC operates far from the surge and choke lines.

6.2.2.2 HPC MATERIALS

The first seven stages blade material was selected as Ti6242 (Ti6Al2Sn4Zr2Mo), and the last three stages were selected as Hastelloy-X. Ti6242 material was used as HPC disk material. The density of Ti6242 was 0.164 lb/in³ whereas elastic modulus and tensile stress were found to be 16680 ksi, and 17400 ksi respect. CAD drawing of the HPC can be seen in Fig. 18.



Figure 19 3-D CAD drawing of the HPC

6.3 COMBUSTION CHAMBERS

Combustion chamber were annular type for Century 250 engine.

6.3.1 Combustion Chambers Material

Ceramic matrix composite (CMC) material was used to manufacture combustion chamber with Zr alloy ceramic coatings. The density of CMC was 0.0722 lb/inc^3 , elastic modulus and tensile stress were obtained as 154.5ksi and 790 ksi, respectively.

6.4 TURBINE DESIGNS

THE CENTURY had 2 stages of HPT and 4 stages of LPT. Similar concept was used to design turbines of the turbofan engines in AxStream software. Table 11 shows the turbine design criteria's which have been reported in the literature. We remarked not to exceed $45 \times 10^9 \text{ in}^2 \times \text{rpm}^2$ in the turbine designs and Zweifel coefficients, loading factors, flow coefficients and reaction numbers were taken in consideration in the turbine designs. Additionally, the AN^2 can be used to check the turbine blade stresses, which is shown in Equation 1. AN^2 rule is a design limit for a turbine material at maximum temperature. Its typical values for traditional turbines are in $0.5 - 10 \times 10^{10} \text{ in}^2 \times \text{RPM}^2$ rang [33].

$$AN^2 = \Omega_{\text{shaft}}^2 \times A \times 30 \pi \quad (1)$$

Table 15 Turbine design parameters

Parameter	Range Of Values	Parameter	Range Of Values
$AN^2 [\text{in}^2 \times \text{rpm}^2]$	HPT: $4-5 \times 10^{10}$ LPT: $<6 \times 10^7$	Zweifel Coefficient	$0.75 < \xi < 1.15$
Turbine Inlet Temperature	$R \leq 3150$	Degree of Reaction at Hub	$0.15 < R < 0.85$
Exit Mach Number	$0.4 < M < 0.5$	Hub to Tip Ratio at Inlet	$2.5-3.5$
Exit Swirl Angle	$0^\circ - 20^\circ$	Aspect Ratio	$0.8 < \psi < 2.5$
Mach Number Between Stages	$0.85 < M < 1.2$	Loading Coefficient	
Flow Coefficient	$0.5 \leq \phi \leq 1.5$		

6.4.1 HIGH PRESSURE TURBINE (HPT) DESIGN

The CENTURY 250 HPT was designed in AxStream through the data that obtained from the GasTurb14. The boundary conditions and geometric data used in HPT design in AxStream are shown in Table 16.

Table 16 Thermodynamic and geometrical data for HPT design.

Thermodynamic and Geometrical Properties			
Total Pressure (inlet) [psi]	552.87	1 st Stage Tip Diameter [inch]	16.62
Total Pressure (outlet) [psi]	187.54	2 nd Stage Tip Diameter [inch]	15.89
Pressure Ratio	2.94	1 st Stage Hub Diameter [inch]	13.06
Total Temperature (inlet) [R]	3000	2 nd Stage Hub Diameter [inch]	12.68
Total Temperature (outlet) [R]	2309.18	1 st Stage Blade Height [inch]	1.78
Mass Flow [lb/s]	93.78	2 nd Stage Blade Height [inch]	1.6
Shaft Rotational Speed [RPM]	23533	Number of Stage	2

2D streamline calculations were performed with the 9 streamline and 500 iterations were done using the find inlet total pressure for given mass flow rate. The annulus and flow path were optimized to obtain higher efficiency than 0.85 and inlet/exit pressure and temperatures in AxStream. Fig. 17 shows 2D flow path, pressure, and Mach number in the HPT. The inlet and exit total pressures were found to be 516.3 psi and 179 psi whereas inlet/exit total temperatures were determined as 3000R/2312R. Moreover, the relative Mach number of the HPT rotor tip exit was 0.94 which was lower than 1.

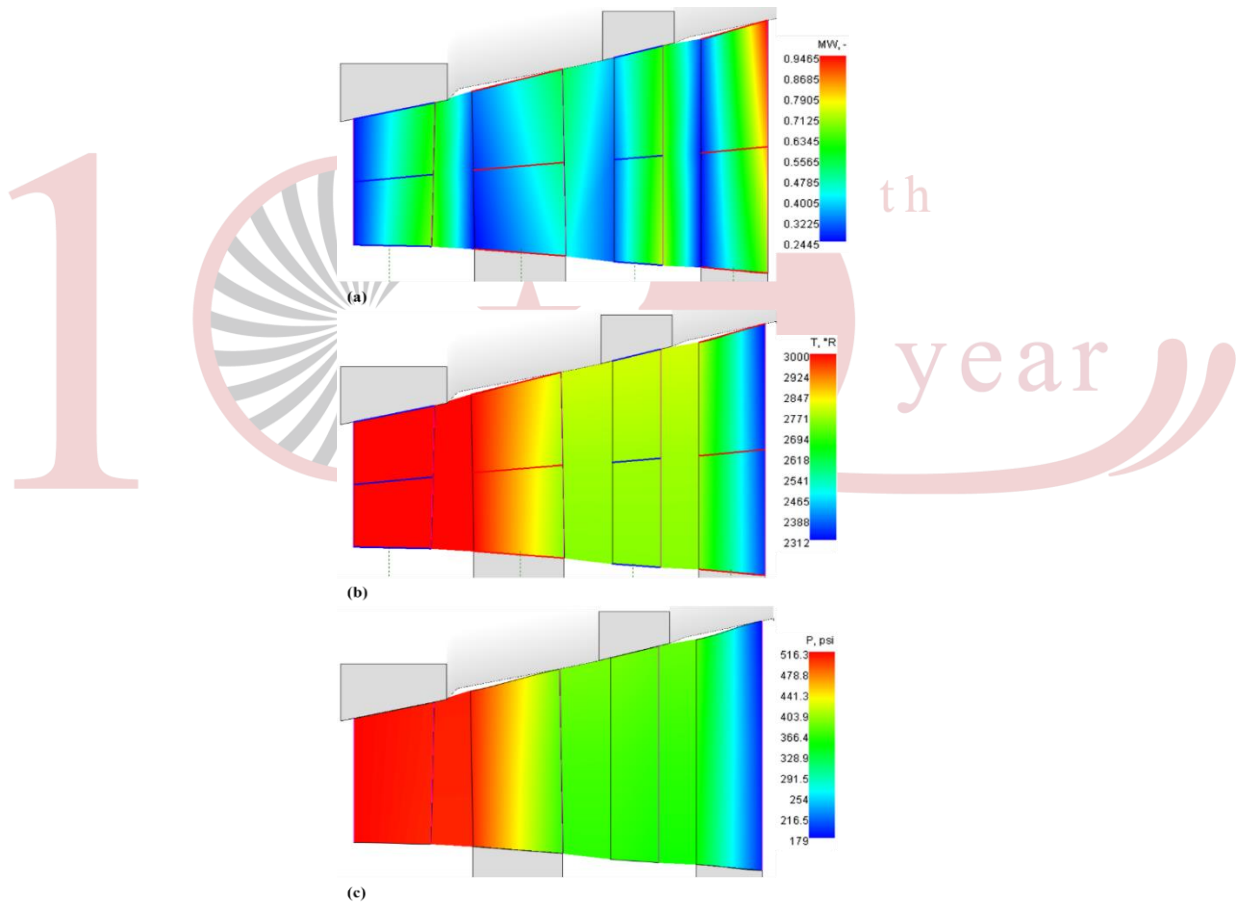


Figure 20 HPT 2D Flow path calculation result (a) Mach number, (b) Total temperature, (c) Total pressure

Fig. 16 shows the velocity triangles of the HPT.

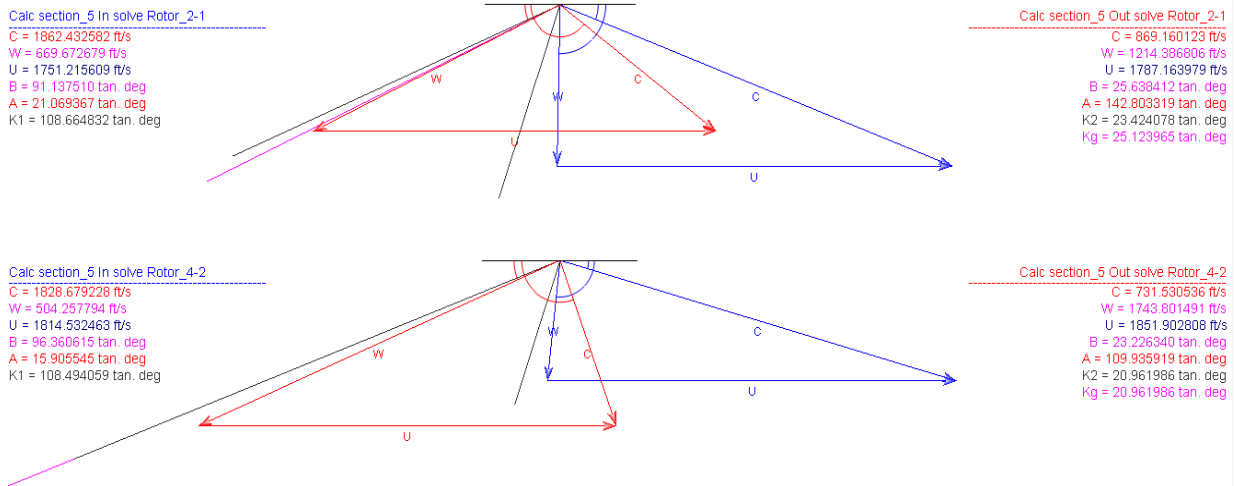


Figure 21 Hub section HPT velocity triangles from AxStream

6.4.1.1 HPT RESULTS

The design results of the HPT were shown in Table 17. It was found that stage loading was in the range of 1.4 and 2.4 and the flow coefficient was 0.7/0.6 which was in the range of 0.6 and 0.9.

Table 17 HPT design results from AxStream

Parameter	STAGE 1		STAGE 2	
	Stator	Rotor	Stator	Rotor
Flow Coefficient	0.7		0.62	
Work Coefficient	1.43		1.8	
Stage Pressure Ratio	1.38		1.98	
Number of Blades	97	83	80	86
Aspect Ratio	1.36	1.58	2.06	2.39
Blade Chord [inch]	0.74	0.82	0.75	0.74
Solidity	1.41	1.45	1.15	1.23
Stagger Angle [tan.deg]	46.72	45.34	65.65	55.22
Leading Edge Radius [in]	0.03	0.02	0.04	0.02
Trailing Edge Radius [in]	0.003	0.004	0.003	0.003
Zweifel Coefficient	0.79	0.75	0.73	0.80
Degree of Reaction at Hub	-	0.36	-	0.39
AN^2 [in ² × rpm ² × 10 ⁶]	39869			

The 3D CAD drawing of the HPT was given in Fig. 21.



Figure 22 3-D CAD drawing of the HPT

6.4.1.2 OFF-DESIGN PERFORMANCE OF HPT

HPT off design performance map was obtained from GasTurb14 and showed in Fig. 22.

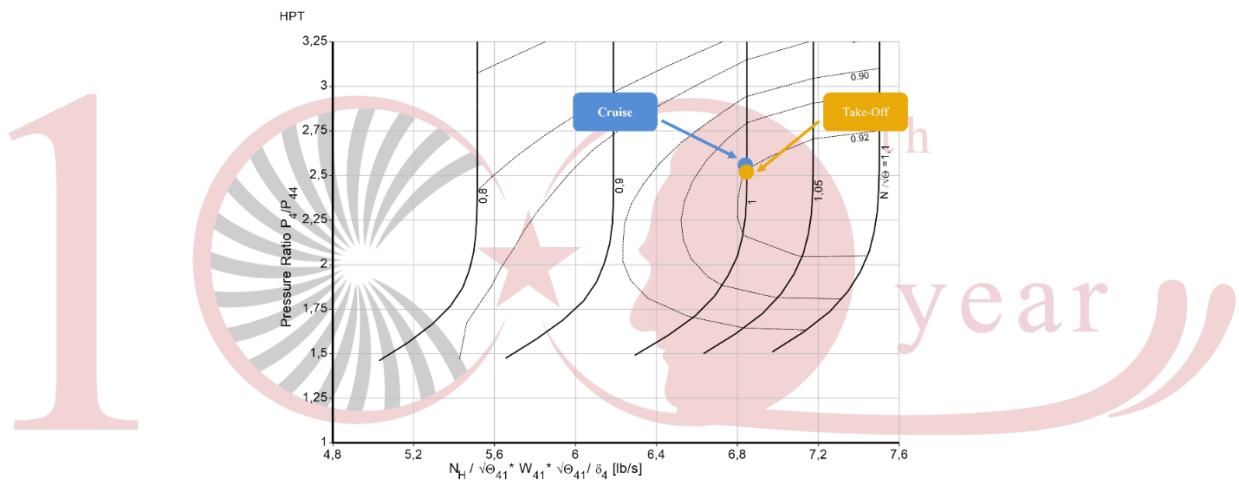


Figure 23 HPT off design performance map

6.4.1.3 HPT MATERIALS

The TMS238 (Ni-based super alloy) was selected as a blade material and composite coatings were used to increase thermal strength of the blades as shown Fig. 20. The HPT disk was also thought to be manufactured from the TMS238.

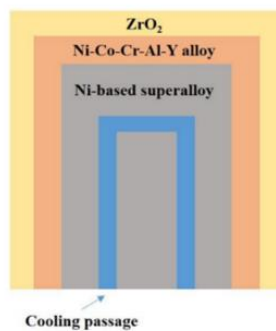


Figure 24 HPT blade material and coatings

6.4.2 LOW PRESSURE TURBINE (LPT) DESIGN

Table 11 shows the data obtained from the GasTurb14 for LPT design.

Table 11 Thermodynamic and geometrical design parameters of the LPT

Thermodynamic and Geometrical Properties			
Total Pressure (inlet) [psi]	183.8	Shaft Rotational Speed [RPM]	10428
Total Pressure (outlet) [psi]	24.7	1 st Stage Tip Diameter [inch]	19.18
Pressure Ratio	7.44	4 th Stage Tip Diameter [inch]	23.74
Total Temperature (inlet) [R]	2294.5	1 st Stage Hub Diameter [inch]	13.68
Total Temperature (outlet) [R]	1481.2	4 th Stage Hub Diameter [inch]	13.54
Mass Flow [lb/s]	104.7	1 st Stage Blade Height [inch]	2.75
Number of Stage	4	4 th Stage Blade Height [inch]	5.1

LPT consisted of 4 axial stages and AxStream streamline calculation module was used to optimize 2D flow path by 9 streamlines. Similar boundary conditions and calculation models with HPT were used in 2D streamline calculations of LPT. Fig. 20 shows LPT flow path optimized in AxStream with Mach number, total temperature, and pressure changes.

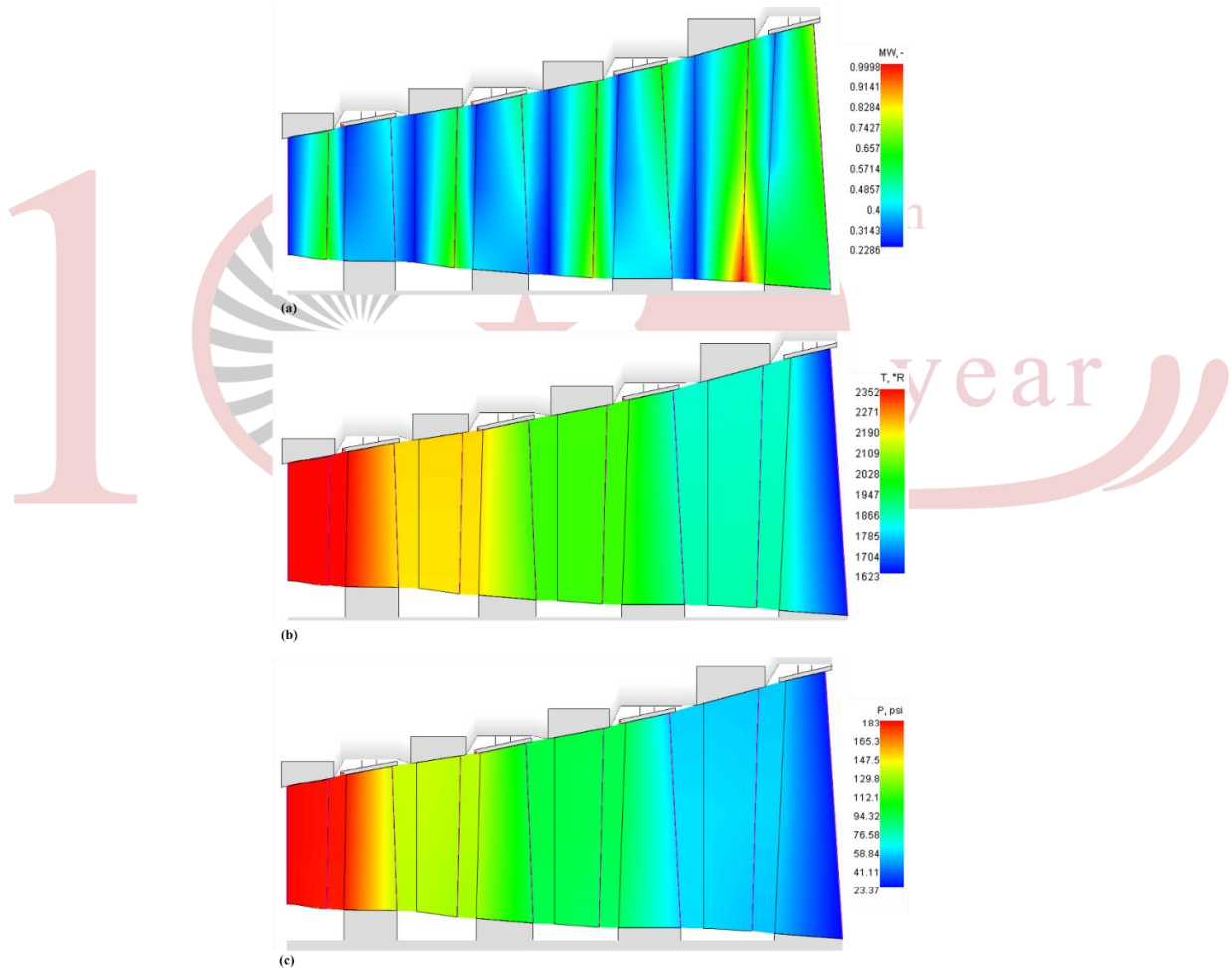


Figure 25 LPT 2D streamline calculation result (a) Relative mach, (b) Total temperature, (c) Total pressure

Velocity triangles of the LPT are illustrated in Fig. 25.

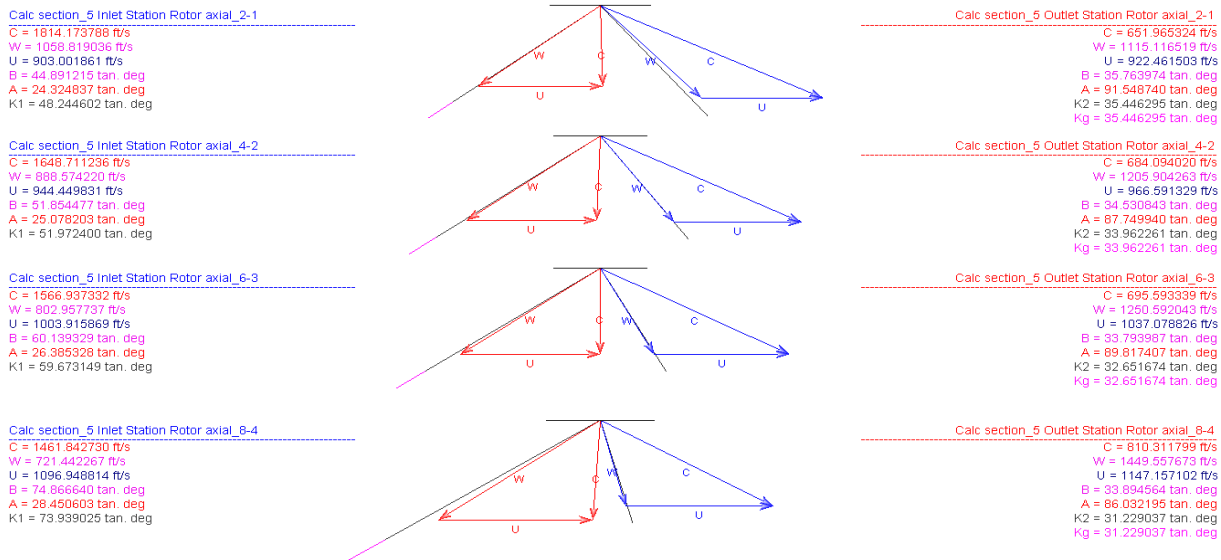


Figure 26 LPT velocity triangles from AxStream

6.4.2.1 LPT RESULTS

LPT design results are presented in Table 12 showing the first and the last stages results. When the results were investigated, it was found that they were in the range of literature.

Table 12 LPT design results

Parameter	STAGE 1		STAGE 4	
	Stator	Rotor	Stator	Rotor
Flow Coefficient	0.6		0.67	
Work Coefficient	1.11		1.32	
Stage Pressure Ratio	1.3		1.64	
Degree of Reaction at Hub	0.15		0.28	
Number of Blades	74	88	66	78
Aspect Ratio	2.26	2.8	3.27	3.99
Blade Chord [in]	1.12	1	1.44	1.3
Solidity	1.31	1.39	1.42	1.5
Stagger Angle [tan.deg]	46.53	19.8	46.59	34.26
Leading Edge Radius [in]	0.05	0.04	0.03	0.05
Trailing Edge Radius [in]	0.005	0.004	0.005	0.005
Zweifel Coefficient	0.85	1.05	0.79	0.97
AN2 [in ² × rpm ² × 10 ⁶]	38869			

3D CAD drawing of the LPT is presented in Fig. 26.



Figure 27 3-D CAD drawing of the LPT

6.4.2.2 OFF-DESIGN PERFORMANCE OF LPT

Off-design performance map of the LPT was presented in Fig. 24 including take off condition.

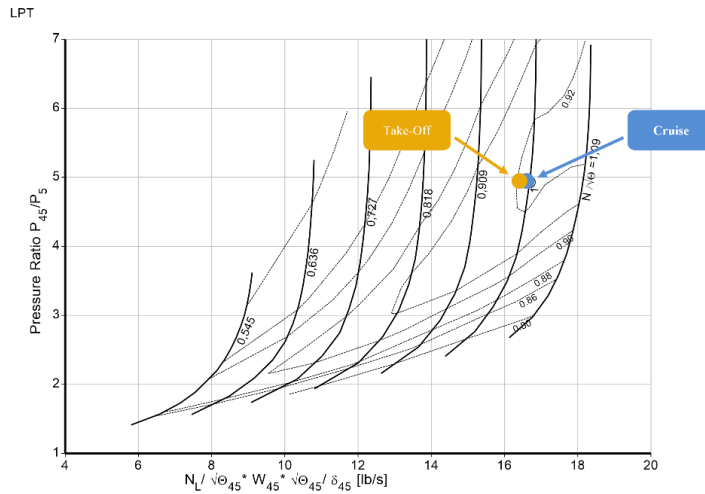


Figure 28 LPT off design performance map

6.4.2.3 LPT MATERIALS

The blade material of the LPT was selected as TMS 238 having the density of 570.24 lb/ft³ and the disk material was similar to blades.

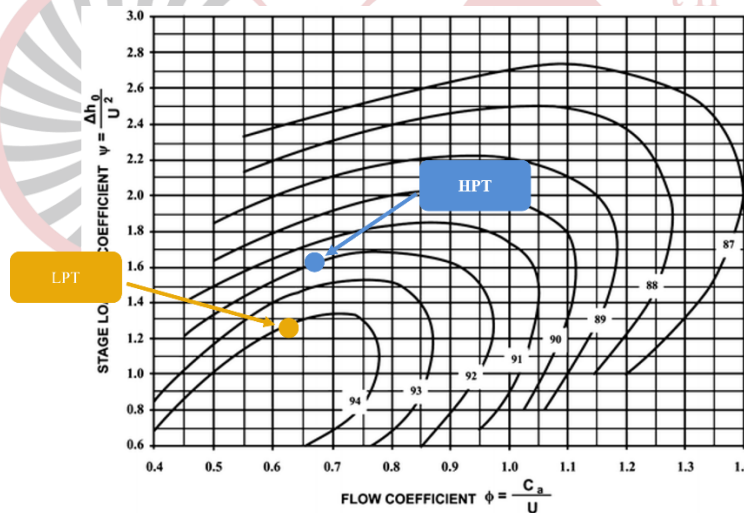


Figure 29 HPT and LPT smith charts

6.5 COLD AND HOT NOZZLE DESIGN

Critical pressure for hot nozzle can be calculated from the Eq.2

$$\frac{P_{06}}{P_c} = \left(\frac{1}{1 - (1/\eta_n) \times (\gamma - 1) / (\gamma + 1)} \right)^{\gamma / (\gamma - 1)} \quad (2)$$

If the nozzle was unchoked $P_8 = P_w$, then the speed of the gases leaving the nozzle given with Eq. 3.

$$V_8 = \sqrt{2 \times C_{ph} \times T_{07} \times \eta_{nt} \times \left[1 - \left(\frac{P_a}{P_{07}} \right)^{(\gamma - 1) / \gamma} \right]} \quad (3)$$

Critical pressure can be calculated by using the Eq.4.

$$\frac{P_{016}}{P_c} = \left(\frac{1}{1 - (1/\eta_n) \times (\gamma - 1) / (\gamma + 1)} \right)^{\gamma / (\gamma - 1)} \quad (4)$$

If the nozzle is unchoked $P_{18} = P_a$, then the speed of the gases leaving the nozzle is given with Eq.5

$$V_{18} = \sqrt{\frac{2 \times \gamma_c \times R \times T_{08} \times \eta_{fn}}{(\gamma_c - 1)} \left[1 - \left(\frac{P_a}{P_{016}} \right)^{\frac{\gamma_c - 1}{\gamma_c}} \right]} \quad (5)$$

The nozzle radius can be calculated at inlet (r_i) or exit (r_e) from the Eq. 6.

$$r = \sqrt{\frac{\dot{m}}{\pi \times \rho \times V}} \quad (6)$$

The axial length of the nozzle can be calculated by using Eq.6 in where θ can be taken in the range of $\theta = 11 - 15^\circ$.

$$L = \frac{r_i - r_e}{\tan \theta} \quad (7)$$

Nozzle material was selected as Inconel 625 whose density is 527 lb/ft³.

6.6 AFT FAN DESIGN

Designed aft fan 2D streamline calculations was shown in Fig. 25. According to the results tip Mach number of the fan was found to be 1.74 which was higher than literature. However, it was thought that this fan will be manufactured a new generation material which is strength for higher stress levels. Inlet and outlet total temperatures and pressures can also be seen in Fig. 25 (b) and (c).

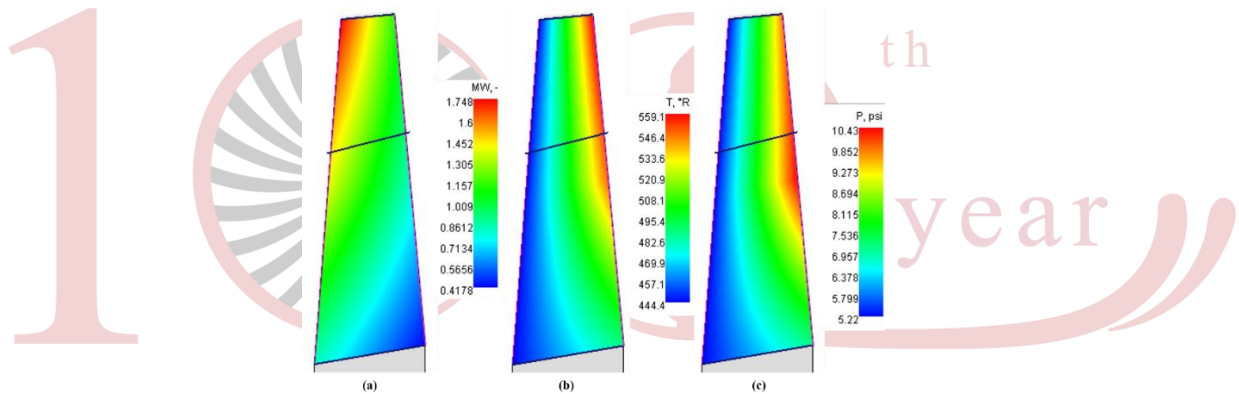


Figure 30 AFT fan 2D streamline calculation result (a) Relative mach, (b) Total temperature, (c) Total pressure

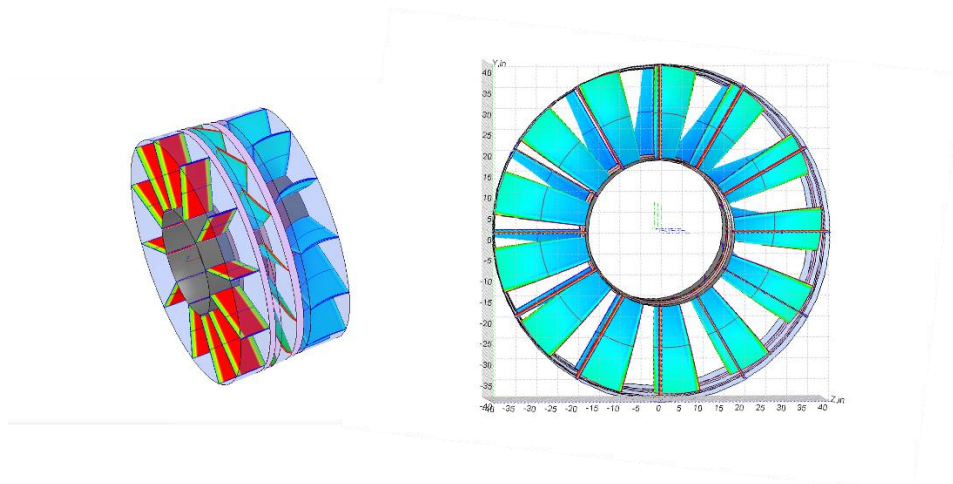


Figure 31 AFT Fan geometry and dimensions from AxStream

7 ENGINE WEIGHT AND GEARBOX WEIGHT CALCULATIONS

Fan rotational speed is recommended nearly one-third of the LPT speed for example (3476/10428 rpm). The LPT rotational speed was 10428 rpm and carried out a gear box usage to reduce fan rotational speed. The gear ratio sun and

the planet gears (z_s) were estimated by equation 8, while the optimum number of planets (N_{rpl}) was calculated by equation 192. The gear ratio was assumed as 3.0 which resulted approximately 3476 rpm fan rotational speed.

$$Nr_{pl} = \frac{16.3677}{2.8 \times \sin^{-1}\left(\frac{z-1}{z+1}\right) \times 1.1736} \quad (8)$$

$$Nr_{pl} = \frac{16.3677}{2.8 \times \sin^{-1}\left(\frac{3-1}{3+1}\right) \times 1.1736} \quad Nr_{pl} = 8.8470$$

$$2 \times z_s^3 + z_s^2 = \frac{0.4 \times z_s^2 + 1}{Nr_{pl}} \quad z_s = 0.27421$$

The weight of the gear box was found by using Eq. 9.

$$W_{gear} = 0.5 \times \frac{W}{K \times \omega} \times \left(\frac{1}{Nr_{pl}} + \frac{1}{Nr_{pl} \times z_s} + z_s + z_s^2 + \frac{0.4 \times z_s^2}{Nr_{pl} \times z_s} + \frac{0.4 \times z_s^2}{Nr_{pl}} \right) \quad (9)$$

$$W_{gear} = 648.6 \text{ lbm}$$

The weight of the Century 250 engine was obtained as 1886.21 lbm without gearbox mass and mass factor added (see Fig. 29). Addition of gearbox mass, net mass was calculated as 2534.81 lbm. When the net mass factor is applied, the total mass of the engine found as 3295.25 lbm. Furthermore, the hybrid propulsion weight was found as 1730.6 lbm, hence the total mass of the hybrid propulsion system was evaluated as 5025.2 lbm. Engine length and dimensions can be seen in Fig. 31. It is found that our engine without electrical system configuration is 37% lighter compared with CFM56-7B24. When the electrical system is taken into consideration, the overall mass of the hybrid-electric propulsion system from the sum of two turbofan engines mass and the electrical system mass, turned out to be 8321 lbm, whereas two CFM56-7B24 engines weight is 10468 lbm. That means our propulsion system is 20% lighter than two CFM56-7B24.

Front LP Shaft Cone Length	in	0,939005
Middle LP Shaft Length	in	43,8321
Middle LP Shaft Radius	in	1,34402
Rear LP Shaft Cone Length	in	2,56719
HP Shaft Cone Length	in	3,91416
HP Shaft Length	in	3,58926
HP Shaft Radius	in	2,02918
Engine Length	in	119,418
Max Engine Diameter	in	87,6661
Nacelle Length (Bypass only)	in	91,8678
LP Shaft Mass	lbm	46,3164
HP Shaft Mass	lbm	8,51944
Gear Box Mass	lbm	0
Net Mass	lbm	1886,21
Total Mass	lbm	1886,21
LP Spool Inertia	lb ² in ²	65177,6
HP Spool Inertia	lb ² in ²	2886,94

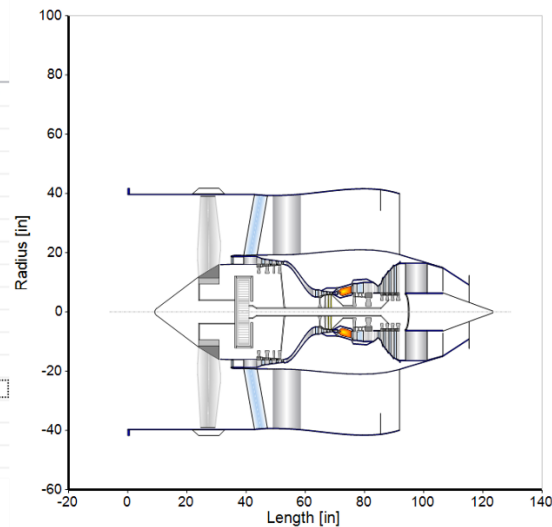


Figure 32 Engine weight and dimensions

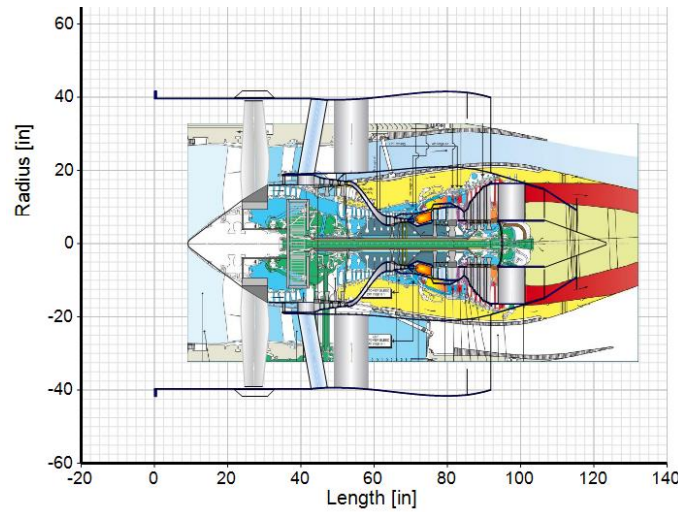


Figure 33 Engine cross section with CFM56-7B24

8 HYBRID PROPULSION SYSTEM DESIGN

Aft fan was designed to ingest boundary air layer and provide additional thrust for plane during the flight. Aft fan was propelled by an electric motor which was powered through the two generators. All two generators also powered by the two primary turbo fan engines which mounted below the wings. The aim of the using aft fan was to ingest boundary layer which formed around the plane body, thus the drag force exerted on the plane body was decreased. Here, we connected the generators to HP spool in our design which resulted in thrust decrease. Fig. 25 shows the designed hybrid propulsion in GasTurb14 software. Aft fan rotational speed was 3500 rpm and needs to 3500 HP at running condition.

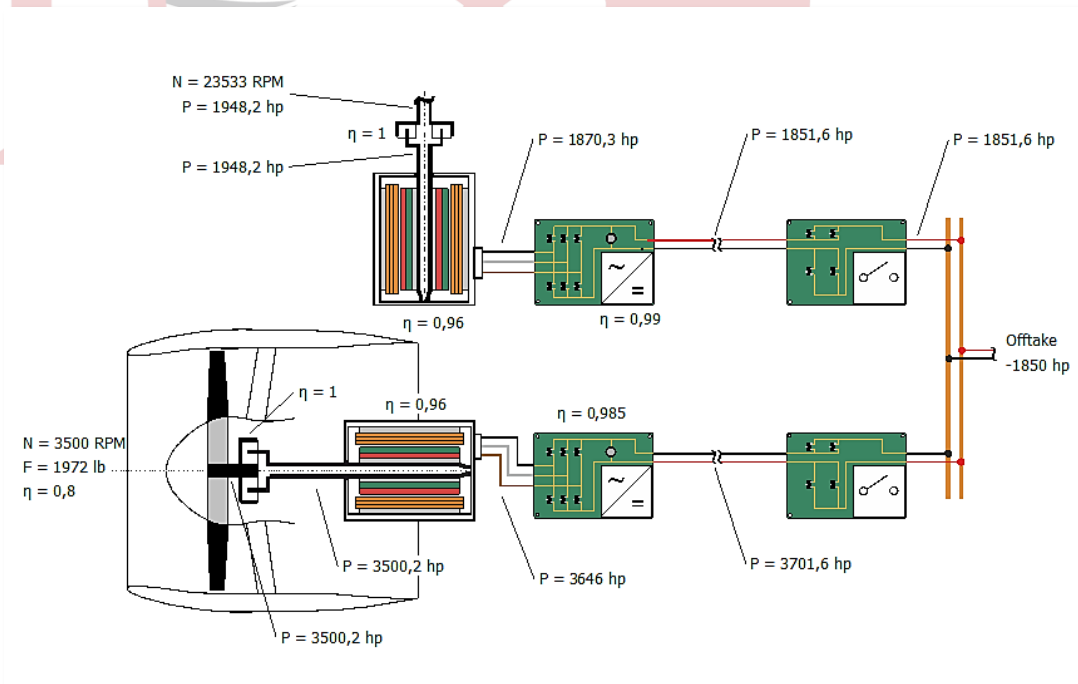


Figure 34 Operation of the hybrid-electric propulsive system

TSFC comparison of the baseline and hybrid-electric showed almost identical fuel consumption. This shows that by using the hybrid-electric propulsion boundary layer ingested and drag force exerted on plane body decreased. However, hybrid-electric propulsion increased the net thrust 10% and when drag force reduction taken consideration fuel consumption will decrease. The aft fan is useful for planes and the loss of energy from the engines is provided more with the help of the aft fan. Even though it causes an increase in mass when added, it allows to catch the flow separation that occurs around the plane body and thanks to the slow air flow around the body, the aircraft can fly at the same speed with less thrust at the same altitude. This constitutes fuel reduction at the cruise condition.

Degree of hybridization (DOH) was calculated by Eq. 10. The DOH number of 0.28 showed that hybridization level was 28% which was a good agreement in the project. This means that %28 of the total thrust was obtained from the electrical aft fan.

$$DoH = \frac{\text{Power Extraction}}{(\text{Power Extraction} + \text{Propulsive Power})}$$

$$\text{Propulsive Power} = \text{Net Thrust} \times \text{Flight Velocity}$$

$$\text{Propulsive Power} = 1971,8 \text{ lb} + 5048 * 2 \text{ lb} = 12067,8 \times 0.8$$

$$\text{Power Extraction} = 1948 \text{ hp} \times 2$$

$$DoH = 0,287 = \%28.7$$

9 MISSION AND PROPULSION COMPARISON

Non hybrid propulsion system fuel consumption was calculated as 38566.51 lbm and illustrated in Table 7 in section 4.2. The hybrid propulsion mission fuel consumption is shown in Table 14 where the fuel consumption decreased to 30370.96 lb. The cruise thrust of the hybrid electric propulsion was determined via calculation of the net thrust of the two baseline engines and addition of aft fan thrust which corresponded to 10000 lb net thrust of the system. As a result, 21.2% fuel saving was achieved when the hybrid propulsion is used. Although hybrid propulsion carried out 1730 lb additional weight to propulsion system, the fuel saving and thrust increase tolerated this weight increase.

Table 14 Flight mission for designed Century-250 with hybrid electric propulsion system

Segment	Altitude (ft)	Mach Number	Thrust (lbf)	TSFC (lbm/lbf*h)	Fuel Flow (lb/s)	Time(min)	Fuel Burned in Segment (lbm)
Taxi Out	0	0.015	3000	0.3	0.256	15	230.4
Take Off	0-10000	0.38	18000	0.48	2.404	3.5	504.84
Climb	10000-35000	0.43	10000	0.47	1.306	11.5	901.14
Cruise	35000	0.8	4032	0.76	0.765	676.2	26128.368
Descend	35000-10000	0.38	10000	0.44	1.242	24.5	1825.74
Approach & Touchdown	10000-0	0.21	14000	0.38	1.498	8	719.04
Taxi In	0	0.015	3000	0.3	0.256	4	61.44
Total						742.7	30370.96

10 CONCLUSIONS

In this project, a hybrid propulsion was designed with the new turbofan engines having ultra-high bypass ratio of 12. The engines were designed with iterative studies by changing T_4 and T_3 temperatures, OPR, and BPRs to obtain best hybrid propulsion system. The results showed that increasing the BPR of baseline engine from 5.3 to 12 decreased the specific fuel consumption significantly not only at takeoff condition but also at cruise condition. Hybrid electric propulsion increased the total thrust of the plane by 12.1% and ingested the boundary layer apart this thrust increase. The weight of the engines was also decreased from 5585 lbm to 3295lbm, however, the diameter of the engine fan increased from 65 inches to 80 inches. On the other hand, total weight of the hybrid propulsion was obtained as 5025lbm. The diameter increase was traded of with fuel saving and thrust increase with weight reduction. Moreover, DOH calculation showed that 28% hybridization was achieved in this project and this ratio carried out very good fuel saving. It is believed that if this ratio increased up to 50%, it would bring out ultimate fuel consumption to the air planes which resulted decrease in carbon foot print. In conclusion, hybrid propulsion provides restricted thrust increase with extremely fuel saving according to the mission results from the viewpoint of propulsion system, however, it is known that boundary layer ingestion will provide decrement in the fuel consumption and additional thrust. This issue can be investigated via computational fluid dynamics (CFD) analysis and results can be discussed detailly.



11 REFERENCES

- [1] Jack D. Mattingly, *Elements of Gas Turbine Propulsion* (1996).
- [2] Meinhard T. Schobeiri, *Gas Turbine Design, Components and System Design Integration* (2017).
- [3] Ahmed F. El-Sayed, (2018). *Aircraft Propulsion and Gas Turbine Engines*.
- [4] Mattingly, J.D., Heiser, W.H., Pratt, D.T. *Aircraft Engine Design Second Edition* (2002).
- [5] H.I.H Saravanamutto, G.F.C. Rogers, H. Cohen, P.V. Straznicky, A.C. Nix, *Gas Turbine Theory* (2017).
- [6] Arthur H. Lefebvre, Dilip R. Ballal, *Gas Turbine Combustion Alternative Fuels and Emissions* (2010)
- [7] M.M Jafari , 'Advances In Nonlinear Stress Analysis of a Stream Analysis of a Stream', *Latin American Applied Research*, 42: 167-175 (2012)
- [8] *The Nickel Insitute, Alloy IN-738 Technical Data ,2020*
- [9] Jeong-Min Lee , 'Life Prediction of IN738LC Considering Creep Damage under Low Cycle Fagitue', *International Journal of Precision Engineering and Manufacturing-Green Technology*, April 2018/311.
- [10] <https://www.specialmetals.com/documents/technical-bulletins/inconel/inconel-alloy-718.pdf> (Date of Access: 03.01.23)
- [11] http://specialmetals.ir/images/technical_info/nickel%20base/Hastelloy%20X.pdf
- [12] Woo-Gon Kim, Song-Nan Yin, *Tension and creep desing stresses of the 'Hastelloy-X alloy for high-temperature gas cooled reactors, Materials Science and Engineering A* 483-484 (2008)
- [13] <https://www.specialmetals.com/documents/technical-bulletins/inconel/inconel-alloy-718.pdf> (Date of Access: 15.02.23)
- [14] Mattingly, J.D. Hever, W.H., "Aircraft Engine Design," J.S. Pr:e11ieuniecki Ed., AIAA, Restou Virginia, 2002.
- [15] Reddy N.M., Tulapurkara, E.G., Ganesan, V. *Analysis of non-reacting and reacting flow inside a jet engine afterburner and parametric studies, Progress in Computational Fluid Dynamics*, 12:5, 2012, 353-362.
- [16] 2023 AIAA Undergraduate Team Engine Design RFP
- [17] Mattingly Jack D., Heiser William. H., Pratt David T., *Aircraft Engine Design, AIAA Education Series, Reston, Virginia, 2nd Edition, 2002*
- [18] <https://inchem.org/documents/icsc/icsc/eics0663.htm> (Date of Access: 12.12.2022)
- [19] Marek Lazazyk, Roman Domanski, " Numerical simulation of thermally loaded aircraft engine turbine blade covered with thermal barrier coating-TBC" *Journal of Kones powertrain and transport*, 19:3, 2012.
- [20] Ahmed F. El-Sayed, (2018). *Aircraft Propulsion and Gas Turbine Engines*
- [21] <https://www.csidesigns.com/uploads/resources/Super-Alloys-Data-Sheet.pdf> (Date of Access: 17.09.2022).
- [22] <https://bircelik.com/tr/kategori/hastelloy-x> (Date of Access: 05.02.2023).
- [23] Muktinutalapati, N.R. (2011). *Materials for Gas Turbines – An Overview, Advances in Gas Turbine Technology, Dr. Ernesto Benini (Ed.)*.
- [24] Dutta, SandipEkkad, SrinathHan, Je-Chin -*Gas Turbine Heat Transfer and Cooling Technology, Second Edition-CRC Press (2012)-Chapter 3: Turbine Film Cooling*
- [25] Nimesh, P.M., Ganesan, Dr. S., Dr. Allamaprabhu C. Y *Prediction of Gas Turbine Afterburner Performance Using CFD, Proceedings of the 1st National Aerospace Propulsion Conference, March 15-17, 2017, IIT Kanpur, 1-8.*
- [26] Farokhi, Saeed, *Aircraft Propulsion, Wiley, 2nd Edition, 2014*

- [27] Ugural, A. C., & Fenster, S. K. (2011). *Advanced mechanics of materials and applied elasticity*. Pearson Education.
- [28] BP Production Data, BP Turbo Oil 2197
- [29] Davide Boiani, "Finite Element Structural and Thermal Analysis of JT9D Turbofan Engine First Stage Turbine Blade", Bachelor Thesis, Alma Mater Studiorum, Bologna, Italy
- [30] KTW Titan Matrix Composite (TMC), <https://ktwtechnology.de/en/products/titan-matrixcomposite/>
- [31] Muktinutalapati Nageswara Rao, "Materials for Gas Turbines – An Overview", VIT University, India
- [32] Kawagishi Kyoko, Yeh An-Chou, Yokokawa Tadaharu, Koyashi Toshiharu, Koizumi Yutaka, Harada Hirsohi, "Development of an Oxidation Resistant High Strength Sixth Generation Single-Crystal Superalloy TMS-238", 12th International Symposium on Superalloys, 2012.
- [33] Pollock T. M., Tin Sammy, "Nickel-Based Superalloys for Advanced Turbine Engines: Chemistry, Microstructure, and Properties", *Journal Of Propulsion*
- [34] Sato Akihiro, Harada Hiroshi, Yeh An-Chau et al., "A 5th Generation Sc Superalloy With Balanced High-Temperature Properties and Processability", TMS (The Minerals, Metals and Materials Society), 2008
- [35] Linke Andreas, Diesinger, *Systems of Commercial Turbofan Engines an Introduction to Systems Functions*, Springer-Verlag Berlin Heidelberg, 1st Edition, 2008
- [36] Titanium Ti-6Al-4V (Grade 5), ASM Aerospace Specifications Metals Inc, <http://asm.matweb.com/search/SpecificMaterial.asp?bassnum=mtp642>, (Accessed on: 2018, March 22)
- [37] Petko Jeanne F., Kiser Douglas, McCue Terry, "Characterization of C/SiC Ceramic Matrix Composites (CMCs) with Novel Interface Fiber Coatings", QSS Group, Inc., Cleveland, Ohio, USA, 2002
- [38] Kurzke, J., & Halliwell, I. (2018). *Propulsion and power: an exploration of gas turbine performance modeling*. Spring
- [39] Liansheng Liu, Datong Liu, Yujie Zhang and Yu Peng, *Effective Sensor Selection and Data Anomaly Detection for Condition Monitoring of Aircraft Engines*, Department of Automation Measurement and Control, Harbin Institute of Technology, Harbin 150001, Published: 29 April 2016
- [40] Kima, D.H., Kim, J.H., Sa, J.A., Lee, Y.S., Park, C.K., Moon, S. *Stress rupture characteristics of Inconel 718 alloy for ramjet combustor*, *Materials Science and Engineering A*, 483–484, (2008), 262–265.
- [41] Lee, Hyeonseok, Seongjun Park, and Jungyun Kim. "Effect of two different gutter shapes on afterburner performance." *Journal of Mechanical Science and Technology*, vol. 32, no. 2, 2018, s. 837-845.
- [42] Bons, J. P., and J. L. Kerrebrock. "Effusion cooling in gas turbine combustion chambers." *Journal of Turbomachinery*, vol. 125, no. 2, 2003, s. 333-347.
- [43] Jasinski, R. *Mass and number analysis of particles emitted during aircraft landing*, *E3S Web of Conferences* 44, 00057, (2018).
- [44] Ali, H. (2018). *Gas Turbine Performance*. John Wiley & Sons
- [45] M. Heitor da Silva, L. Leandro, H. Santos, and F. Silva. *Assessment of Spray Characterization Methods for an Aeronautical Plain Orifice Atomizer*. *Atomization and Sprays*, 2016.
- [46] Meherwan P. Boyce. *Gas Turbine Engineering Handbook*. Elsevier, Fourth edition, 2012. Sayfa 124.
- [47] Cumpsty, N. A. *Jet Propulsion: A Simple Guide to the Aerodynamic and Thermodynamic Design and Performance of Jet Engines*. Cambridge University Press, 2003. p. 8.
- [48] Henderson, D. *Introduction to Aerospace Propulsion*. John Wiley & Sons, 2010. p. 177.
- [49] ANSYS Inc. *ANSYS Fluent User's Guide*. ANSYS Inc., Canonsburg, PA, 2019. p. 2575
- [50] J.A. Lovett, *Development needs for advanced afterburner desings*, In *Proceedings of 40th AIAA/ASME/SAE/ASEE Joint Propulsion Conference and Exhibit*, Fort Lauderdale, Florida, US, 2004.

Station	W	T	P	WRstd		
amb	lb/s	R	psia	lb/s	FN	= 24601,31 lb
2	983,441	523,97	14,696		TSFC	= 0,1875 lb/(lb*h)
13	921,923	522,00	14,504	999,666	WF	= 1,28105 lb/s
21	61,518	563,27	18,619	758,299	s NOX	= 1,8219
22	61,518	566,35	18,520	51,011		
24	61,518	566,35	18,334	51,527	Core Eff	= 0,4634
25	61,518	659,93	29,515	34,551	Prop Eff	= 0,0000
3	60,288	659,93	28,925	35,256	BPR	= 14,9862
31	54,751	1619,57	556,952	2,811	P2/P1	= 1,0000
4	56,032	1619,57	556,952		P3/P2	= 38,40
405	58,493	2995,14	534,674	3,701	P5/P2	= 1,1789
41	60,031	2941,64	534,674		NGV Out.	2 Stage HPT
43	60,031	2910,34	534,674	3,908	P16/P13	= 0,9800
44	61,569	2061,18	97,418		P16/P6	= 1,06717
45	62,594	2050,74	97,418		P16/P2	= 1,25809
49	62,594	2038,54	95,069	19,182	P6/P5	= 1,00000
5	62,799	1391,57	17,099		A8	= 390,06 in ²
8	62,799	1391,41	17,099	88,404	A18	= 2954,47 in ²
18	921,923	563,27	18,247	773,774	XM8	= 0,47894
Bleed	0,000	1619,57	556,952		XM18	= 0,56483
					WBld/w2	= 0,00000
					CD8	= 0,92852
					CD18	= 0,94149
					PWX	= 200,0 hp
					V18/v8_id	= 0,75632
					WBLD/w22	= 0,00000
					wreci/w25	= 0,00000
					Loading	= 100,00 %
					WCHN/w25	= 0,06500
					WCHR/w25	= 0,02500
					WCLN/w25	= 0,01667
					WCLR/w25	= 0,00333
					WBLD/w25	= 0,00000
					WkBy/w25	= 0,00000
					wkLP/w25	= 0,00000
Efficiency	isent	polytr	RNI	P/P		
Outer LPC	0,9344	0,9367	0,979	1,284		
Inner LPC	0,8500	0,8551	0,979	1,277		
IP Compressor	0,8788	0,8866	1,124	1,610		
HP Compressor	0,8545	0,8989	1,478	19,255		
Burner	0,9995			0,960		
HP Turbine	0,8965	0,8760	4,856	5,488		
LP Turbine	0,9203	0,9026	1,299	5,560		
HP Spool mech Eff	0,9900	Nom Spd	18613 rpm			
LP Spool mech Eff	0,9900	Nom Spd	4461 rpm			
P22/P21=0,9900	P25/P24=0,9800	P45/P44=0,9759				

hum [%]	war0	FHV	Fuel
0,0	0,00000	18413,0	Generic

	Units	St 2	St 22	St 24	St 25	St 3	St 4	St 44	St 45	St 5	St 6	St 8	St 13	St 16	St 18
Mass Flow	lb/s	983,441	61,5181	61,5181	61,5181	60,2877	56,0322	61,5688	62,5941	62,7991	62,7991	921,923	921,923	921,923	
Total Temperature	R	522	566,353	659,934	659,934	1619,57	2995,14	2050,74	2038,54	1391,41	1391,41	1391,41	563,274	563,274	563,274
Static Temperature	R	475,336	539,481	639,584	636,528	1602,15	2990,81	1989,84	2000,23	1376,83	1344,39	1338,37	531,212	536,532	529,558
Total Pressure	psia	14,5038	18,3344	29,515	28,9247	556,952	534,674	97,418	95,0693	17,0985	17,0985	17,0985	18,6194	18,247	18,247
Static Pressure	psia	10,4553	15,4573	26,4407	25,4797	534,136	531,237	85,8069	87,7755	16,411	14,9551	14,696	15,1602	15,3835	14,696
Velocity	ft/s	748,26	569,293	495,429	531,327	480,843	257,38	938,057	743,801	441,719	793,237	842,466	621,418	567,739	637,182
Area	in ²	3187,95	201,215	160,249	154,317	20,0645	65,3892	81,203	102,312	636,353	379,692	362,177	2773,47	3021,58	2781,62
Mach Number		0,7	0,5	0,4	0,43	0,25	0,1	0,442538	0,35	0,247795	0,45	0,478937	0,55	0,5	0,56483
Density	lb/ft ³	0,059367	0,077334	0,11158	0,108041	0,89983	0,479422	0,116392	0,118444	0,032172	0,030025	0,029637	0,077028	0,077388	0,074903
Spec Heat @ T	BTU/(lb*R)	0,240096	0,240457	0,241538	0,241538	0,267889	0,306036	0,288244	0,287796	0,268795	0,268795	0,268795	0,240422	0,240422	0,240422
Spec Heat @ Ts	BTU/(lb*R)	0,239947	0,240151	0,241303	0,241268	0,267375	0,305979	0,28682	0,286901	0,26829	0,267168	0,266696	0,240125	0,240142	0,24012
Enthalpy @ T	BTU/lb	-3,51762	7,15061	29,7068	29,7068	272,972	685,255	402,221	398,51	218,021	218,021	218,021	6,40826	6,40826	6,40826
Enthalpy @ Ts	BTU/lb	-14,7065	0,673935	24,8018	24,0652	268,351	683,931	384,637	387,455	214,122	205,447	203,837	-1,30874	-0,033111	-1,70523
Entropy Function @ T		-0,096874	0,188954	0,725979	0,725979	4,01641	6,74911	5,09062	5,06326	3,51409	3,51409	3,51409	0,169805	0,169805	0,169805
Entropy Function @ Ts		-0,424177	0,018257	0,615984	0,599165	3,97458	6,74266	4,9637	4,98344	3,47305	3,38015	3,36268	-0,035729	-8,9946E-4	-0,046626
Exergy	BTU/lb	-0,472263	8,34613	28,713	27,9867	259,294	571,877	287,256	283,651	97,1784	97,1784	97,1784	8,84676	8,12052	8,12052
Gas Constant	BTU/(lb*R)	0,068607	0,068607	0,068607	0,068607	0,068607	0,068606	0,068606	0,068606	0,068606	0,068606	0,068606	0,068607	0,068607	0,068607
Fuel-Air-Ratio		0	0	0	0	0	0,023398	0,021249	0,020894	0,020824	0,020824	0,020824	0	0	0
Water-Air-Ratio		0	0	0	0	0	0	0	0	0	0	0	0	0	0
Inner Radius	in	10,018	13,4975	13,7369	7,27146	7,45749	8,63499	8,63499	8,63499	8,63499	8,63499	5,07334	15,4681	20,4225	19,9374
Outer Radius	in	33,3934	15,6918	15,4826	10,0992	7,87677	9,76612	10,0205	10,3504	16,6469	13,9794	12,2433	33,4976	37,1332	36,5778
Axial Position	in	16,6967	16,6967	29,9446	38,8736	51,3227	58,385	61,0997	63,2584	72,1784	88,3259	98,1115	36,5979	69,4769	72,1428

Engine 2 Take Off Cycle Results.

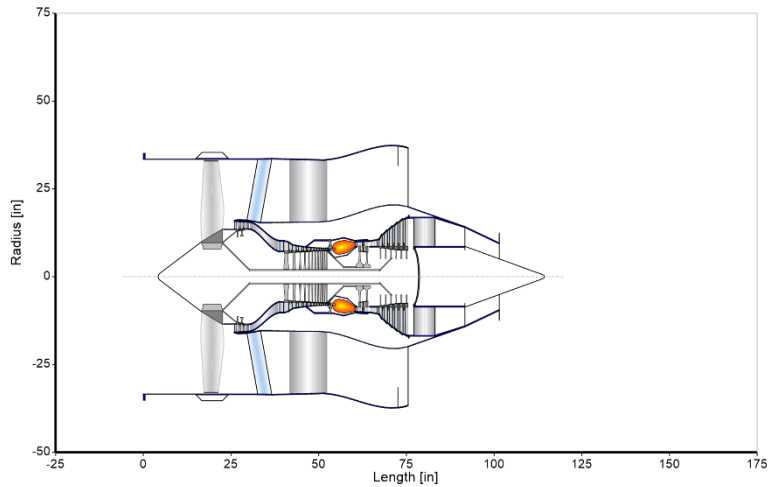
Station	W lb/s	T R	P psia	WRstd lb/s	FN	
amb		393,85	3,458		=	3953,70 lb
2	434,405	444,38	5,273	1120,701	=	0,5890 lb/(lb*h)
13	408,454	478,30	6,645	867,466	=	0,64688 lb/s
21	25,952	480,04	6,612	55,494	=	1,1340
22	25,952	480,04	6,533	56,159	=	2,2434 EPR
24	27,659	604,40	12,479	35,162	=	Core Eff = 0,5503
25	28,180	604,40	12,221	36,582	=	Prop Eff = 0,8449
3	27,617	1562,01	256,837	2,742	=	BPR = 15,7390
31	25,080	1562,01	256,837		=	P2/P1 = 1,0000
4	25,727	3070,12	247,060	3,723	=	P3/P2 = 48,71
405	26,854	3011,96	247,060		=	P5/P2 = 2,2434
41	27,559	2977,87	247,060	3,928	=	NGV Out. 2 Stage HPT
43	27,559	2134,64	46,929		=	P16/P13 = 0,9738
44	28,263	2121,19	46,929		=	P16/P6 = 0,54706
45	28,733	2107,12	45,867	18,556	=	P16/P2 = 1,22728
49	28,733	1572,21	11,829		=	P6/P5 = 1,00000
5	28,827	1571,32	11,829	62,336	=	A8 = 390,06 in ²
8	28,827	1571,32	11,829	62,336	=	A18 = 2954,47 in ²
18	408,454	478,30	6,471	890,780	=	XM8 = 1,00000
Bleed	0,000	1562,01	256,836		=	XM18 = 0,98981
					=	WBld/w2 = 0,00000
					=	CD8 = 0,94356
					=	CD18 = 0,97035
Efficiency	isentr	polytr	RNI	P/P		PWx = 200,0 hp
Outer LPC	0,8962	0,8996	0,431	1,260		v18/v8_id = 0,40649
Inner LPC	0,8334	0,8386	0,431	1,254		WBLD/w22 = 0,00000
IP Compressor	0,7831	0,8019	0,487	1,910		Wrecj/w25 = 0,00000
HP Compressor	0,8258	0,8804	0,693	21,017		Loading = 205,27 %
Burner	0,9984			0,962		WCHN/w25 = 0,06500
HP Turbine	0,8940	0,8738	2,184	5,265		WCHR/w25 = 0,02500
LP Turbine	0,9068	0,8914	0,603	3,878		WCLN/w25 = 0,01667
						WCLR/w25 = 0,00333
HP Spool mech Eff	0,9900	Speed	18613 rpm			WBLD/w25 = 0,00000
LP Spool mech Eff	0,9900	Speed	5353 rpm			WLkBy/w25 = 0,00000
						WlKLP/w25 = 0,00000
P22/P21=0,9882	P25/P24=0,9793	P45/P44=0,9774				

hum [%]	war0	FHV	FueJ
0,0	0,00000	18413,0	Generic

Units	St 2	St 22	St 24	St 25	St 3	St 4	St 44	St 45	St 5	St 6	St 8	St 13	St 16	St 18
Mass Flow	lb/s	434,405	25,9517	27,6593	28,1801	27,6165	25,7272	28,2634	28,7331	28,827	28,827	408,454	408,454	408,454
Total Temperature	R	444,378	480,044	604,401	604,401	1562,01	3070,12	2121,19	2107,12	1571,32	1571,32	478,302	478,302	478,302
Static Temperature	R	370,172	450,935	584,966	580,91	1546,08	3065,68	2063,07	2070,52	1563,59	1548,27	1343,18	435,973	443,948
Total Pressure	psia	5,27271	6,53344	12,4791	12,2206	256,837	247,06	46,9294	45,8667	11,8288	11,8288	11,8288	6,64498	6,47106
Static Pressure	psia	2,78418	5,25032	11,1259	10,6324	246,848	245,454	41,7327	42,5957	11,5976	11,15	6,35714	4,80659	4,98697
Velocity	ft/s	943,589	590,994	484,161	532,3	459,932	262,175	917,981	728,303	325,836	562,456	1761,14	712,667	642,028
Area	in ²	3187,95	201,215	160,249	154,317	20,0645	65,3892	81,203	102,312	636,353	379,692	184,512	2773,47	3021,58
Mach Number		1	0,5676	0,408536	0,450705	0,243162	0,100719	0,425928	0,337312	0,17227	0,298747	1	0,696073	0,621435
Density	lb/ft ³	0,0203	0,031426	0,051335	0,049401	0,430934	0,216104	0,054599	0,055527	0,02002	0,019438	0,012775	0,029757	0,030319
Spec Heat @ T	BTU/(lb*R)	0,239848	0,239962	0,240897	0,240897	0,266192	0,30836	0,290912	0,290396	0,275574	0,275574	0,239956	0,239956	0,239956
Spec Heat @ Ts	BTU/(lb*R)	0,239612	0,239869	0,240672	0,240626	0,265722	0,308306	0,289536	0,289531	0,275321	0,27482	0,267903	0,239821	0,239876
Enthalpy @ T	BTU/lb	-22,1298	-13,5776	16,3215	16,3215	257,702	710,727	423,784	419,491	267,612	267,612	267,612	-13,9953	-13,9953
Enthalpy @ Ts	BTU/lb	-39,9226	-20,5575	11,637	10,6592	253,474	709,354	406,944	408,891	265,491	261,29	205,63	-24,145	-22,2327
Entropy Function @ T		-0,659571	-0,38973	0,417289	0,417289	3,87641	6,88168	5,24696	5,21632	4,00564	4,00564	4,00564	-0,402436	-0,402436
Entropy Function @ Ts		-1,29816	-0,608374	0,302511	0,278071	3,83675	6,87516	5,1296	5,14234	3,9859	3,94654	3,38468	-0,72631	-0,662949
Exergy	BTU/lb	12,1144	19,1682	44,7466	44,181	274,38	645,171	357,517	353,432	197,648	197,648	19,5512	18,8346	18,8346
Gas Constant	BTU/(lb*R)	0,068607	0,068607	0,068607	0,068607	0,068607	0,068606	0,068606	0,068606	0,068606	0,068606	0,068606	0,068607	0,068607
Fuel-Air-Ratio		0	0	0	0	0	0,025792	0,023424	0,023032	0,022955	0,022955	0	0	0
Water-Air-Ratio		0	0	0	0	0	0	0	0	0	0	0	0	0

Engine 2 Cruise Cycle Results.

Front LP Shaft Cone Length	in	7,73063
Middle LP Shaft Length	in	37,1597
Middle LP Shaft Radius	in	1,99519
Rear LP Shaft Cone Length	in	3,26085
HP Shaft Cone Length	in	4,82022
HP Shaft Length	in	3,68099
HP Shaft Radius	in	2,64163
Engine Length	in	114,132
Max Engine Diameter	in	78,6542
Nacelle Length (Bypass only)	in	75,4826
LP Shaft Mass	lbm	48,1634
HP Shaft Mass	lbm	12,7086
Gear Box Mass	lbm	0
Net Mass	lbm	2713,15
Total Mass	lbm	3527,1
LP Spool Inertia	lb*in ²	93964
HP Spool Inertia	lb*in ²	10196



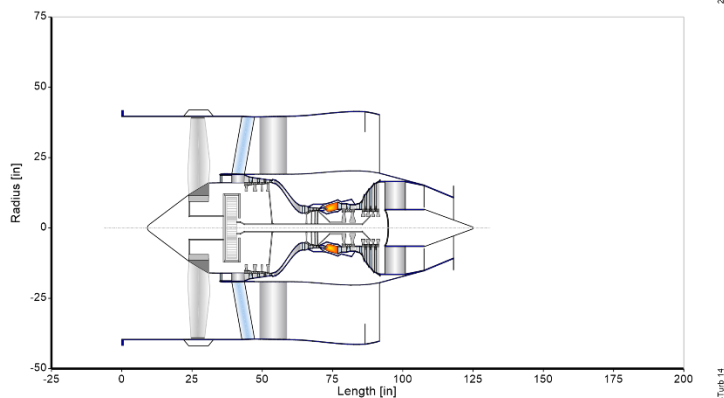
Engine 2 Geometry

Station	W	T	P	WRstd		
amb		R	psia	lb/s	FN	= 5711,10 lb
2	649,779	393,85	3,458		TSFC	= 0,6029 lb/(lb*h)
13	611,812	444,38	5,220	1693,267	WF	= 0,95640 lb/s
21	37,967	478,87	6,494	1330,263	s NOX	= 1,1930
22	37,967	508,82	7,769	71,133	P5/P2	= 2,6613 EPR
24	40,321	508,82	7,670	72,049	Core Eff	= 0,5777
25	41,323	929,77	41,061	19,321	Prop Eff	= 0,8495
3	40,496	1586,71	244,412	4,259	BPR	= 16,1142
31	36,777	1586,71	244,412		P2/P1	= 0,9900
4	37,734	3112,39	234,563	5,791	P3/P2	= 46,82
405	39,387	3053,77	234,563		P5/P2	= 2,6613
41	40,420	3019,23	234,563	6,110	NGV Out. 2 Stage HPT	
43	40,420	2436,00	82,624		P16/P13	= 0,9722
44	41,453	2416,31	82,624		P16/P6	= 0,46210
45	42,142	2399,97	80,950	16,457	P16/P2	= 1,20952
49	42,142	1609,51	13,892		P6/P5	= 0,98352
5	42,279	1608,84	13,892	78,772	A8	= 489,70 in ²
8	42,279	1608,84	13,663	80,092	A18	= 4286,62 in ²
18	611,812	478,87	6,314	1368,358	XM8	= 1,00000
Bleed	0,000	1586,71	244,412		XM18	= 0,96842
					WBld/w2	= 0,00000
					CD8	= 0,95744
					CD18	= 0,97206
Efficiency	isent	polytr	RNI	P/P	PWX	= 200,0 hp
Outer LPC	0,8309	0,8361	0,426	1,244	V18/V8_id	= 0,37658
Inner LPC	0,8309	0,8401	0,426	1,488	WBLD/w2	= 0,00000
IP Compressor	0,7349	0,7878	0,534	5,353	wreci/w25	= 0,00000
HP Compressor	0,8800	0,9043	1,367	6,068	Loading	= 192,52 %
Burner	0,9986			0,960	WCHN/w25	= 0,06500
HP Turbine	0,9165	0,9067	2,041	2,839	WCHR/w25	= 0,02500
LP Turbine	0,9581	0,9483	0,917	5,827	WCLN/w25	= 0,01667
HP Spool mech Eff	0,9900			22238 rpm	WCLR/w25	= 0,00333
LP Spool mech Eff	0,9900			4397 rpm	WBLD/w25	= 0,00000
IPC & LPT				15390 rpm	WLkBy/w25	= 0,00000
					WlKLP/w25	= 0,00000
P22/P21=0,9873	P25/P24=0,9810	P45/P44=0,9797				
hum [%]	war0	FHV	Fuel			
0,0	0,00000	18552,4	Generic			

Units	St 2	St 22	St 24	St 25	St 3	St 4	St 44	St 45	St 5	St 6	St 8	St 13	St 16	St 18
Mass Flow	lb/s	649,779	37,967	40,3208	41,3228	40,4964	37,7337	41,4528	42,1415	42,2792	42,2792	611,812	611,812	611,812
Total Temperature	R	444,378	508,822	929,765	929,765	1586,71	3112,39	2416,31	2399,97	1608,84	1608,84	478,871	478,871	478,871
Static Temperature	R	370,172	474,353	903,693	895,053	1569,49	3107,81	2326,82	2355,78	1586,06	1590,61	1376,28	430,665	440,459
Total Pressure	psia	5,21998	7,67033	41,0613	40,2791	244,412	234,563	82,6243	80,9499	13,8918	13,6628	13,6628	6,49445	6,31365
Static Pressure	psia	2,75633	6,00254	37,043	35,1076	234,309	233,011	70,1785	74,6882	13,1217	13,0543	7,34727	4,48215	4,71365
Velocity	ft/s	943,589	643,103	569,442	656,201	478,116	266,325	1152,85	810,63	559,189	500,151	1781,31	760,533	678,893
Area	in ²	4783,51	248,911	92,1606	85,6546	30,2693	100,819	63,6034	87,481	487,577	549,521	237,199	4123,85	4492,76
Mach Number		1	0,602247	0,388303	0,449544	0,250997	0,101647	0,505223	0,353125	0,293685	0,262325	1	0,747378	0,659709
Density	lb/ft ³	0,020097	0,034154	0,110636	0,105868	0,402943	0,202368	0,081407	0,085573	0,02233	0,022152	0,014409	0,028091	0,028885
Spec Heat @ T	BTU/(lb*R)	0,239848	0,240054	0,246906	0,246906	0,26692	0,308987	0,297106	0,296606	0,276876	0,276876	0,276876	0,239958	0,239958
Spec Heat @ Ts	BTU/(lb*R)	0,239612	0,239944	0,246162	0,245951	0,266413	0,308932	0,295419	0,295791	0,276131	0,27628	0,269128	0,239805	0,239836
Enthalpy @ T	BTU/lb	-22,1298	-6,67727	95,5061	95,5061	264,255	724,034	510,721	505,59	277,965	277,965	277,965	-13,8589	-13,8589
Enthalpy @ Ts	BTU/lb	-39,9226	-14,9423	89,026	86,901	259,686	722,616	484,161	492,458	271,716	272,966	214,554	-25,4178	-32,0263
Entropy Function @ T		-0,659571	-0,186239	1,9433	1,9433	3,93711	6,9453	5,80657	5,77425	4,10089	4,10089	4,10089	-0,398281	-0,398281
Entropy Function @ Ts		-1,29816	-0,431415	1,84031	1,80588	3,8949	6,93866	5,64331	5,69375	4,04385	4,05532	3,48054	-0,769126	-0,690531
Exergy	BTU/lb	11,8428	24,9048	114,879	114,36	277,953	655,356	444,617	439,805	209,771	209,322	209,322	18,9562	18,1933
Gas Constant	BTU/(lb*R)	0,068607	0,068607	0,068607	0,068607	0,068607	0,068607	0,068606	0,068606	0,068606	0,068606	0,068606	0,068607	0,068607
Fuel-Air-Ratio		0	0	0	0	0	0,026005	0,023617	0,023222	0,023145	0,023145	0,023145	0	0
Water-Air-Ratio		0	0	0	0	0	0	0	0	0	0	0	0	0

Engine 4 Cruise Cycle Results

Front LP Shaft Cone Length	in	0,939005
Middle LP Shaft Length	in	43,4589
Middle LP Shaft Radius	in	1,41809
Rear LP Shaft Cone Length	in	2,62535
HP Shaft Cone Length	in	4,16575
HP Shaft Length	in	4,4219
HP Shaft Radius	in	2,03461
Engine Length	in	124,872
Max Engine Diameter	in	87,6706
Nacelle Length (Bypass only)	in	91,6964
LP Shaft Mass	lbm	47,4415
HP Shaft Mass	lbm	9,71954
Gear Box Mass	lbm	0
Net Mass	lbm	2431,47
Total Mass	lbm	2431,47
LP Spool Inertia	lb*in ²	73717,3
HP Spool Inertia	lb*in ²	3068,12



Engine 4 Geometry

100th year